INVESTIGATION OF HYDROGEOCHEMICAL PROCESSES OF GROUNDWATER AT ROYAL BAFOKENG PLATINUM MINE IN THE BUSHVELD IGNEOUS COMPLEX, SOUTH AFRICA

By: Masego Lencwane

(Student number: 483350)

A Research Report submitted to the Faculty of Science, University of the Witwatersrand, Johannesburg, in partial fulfilment of the requirements for the degree of Master of Science in Hydrogeology

UNIVERSITY OF THE
WITWATERSRAND,
JOHANNESBURG

Supervisor: Professor Tamiru Abiye

Johannesburg, 2021

DECLARATION

I declare that this research report is my own, unaided work. It is being submitted for the Master of Science degree in Hydrogeology at the University of the Witwatersrand, Johannesburg. It has not been submitted before for any degree or examination at any other university.

_____

Masego Lencwane 2021/03/23

ABSTRACT

This study was conducted in a platinum mining area to investigate the hydrogeochemical processes that influence groundwater chemistry. Information on the physicochemical properties of the groundwater was obtained from the mine's database. The data were collected quarterly from monitoring boreholes for eight years (from 2007 to 2014). Furthermore, six underground workplaces that experienced water challenges were investigated to identify the source of water and come up with suitable solutions to deal with water challenges. For this part of the investigation, water samples were collected in March 2019 and were used to measure the physicochemical and chemical parameters.

Water-rock interaction, bivariate plot analysis and water type classification were used in the study. The study revealed that the magnesium bicarbonate water type is the most dominant, followed by the magnesium sulphate water type and then mixed water type. The dissolution of fluorite was confirmed from saturation index results and this was supported by the trends in bivariate plots, as well as stoichiometric ratios. Dissolution, mixing and silicate weathering were recognised as processes, which take place in the groundwater system around RBplat and this was confirmed by a Durov plot. Saturation index results indicated precipitation of calcite, owing to its oversaturation. Silicate and carbonate weathering were also identified as processes contributing to the high concentrations of ions in the groundwater system.

Based on the stable isotopes (deuterium and oxygen 18) results, the source of water in the underground workings originates from moisture that circulates regionally and recharged with minimal evaporation effects. This water shows a similar isotopic composition to the local precipitation. The municipal water supply from the underground tap deviates from the other samples and the PMWL, this confirms that there is no leak of the pipes and the other samples are of direct recharge from precipitation.

Keywords: Hydrogeochemical processes, Silicate weathering, Sulphate reduction, Water-rock interaction, Bushveld Igneous Complex.

ACKNOWLEDGEMENTS

My sincere gratitude to Professor Tamiru Abiye for the guidance from the beginning to the end of the project. Thank you Prof for your patience and all the knowledge you've imparted. I would like to thank Royal Bafokeng Platinum Mine for allowing me to use their company as my study area and all the data they have provided.

A big thank you to my colleagues for the motivation and the assistance they have given throughout the project. Thank you to all my classmates for the assistance and motivation throughout the course of the project. I have gained brothers and sisters for life.

To my family and friends, Ke a leboga, ke leboga go menagane. Ke lebogela tshegetso ya lona le thotloetso go tloga ko tshimologong go fitlha mo bokhutlong. Thank you for believing in me even when I did not believe in myself**.**

TABLE OF CONTENTS

LIST OF FIGURES

LIST OF TABLES

NOMENCLATURE

BIC	Bushveld Igneous Complex
BRPM	Bafokeng Rasimone Platinum Mine
DWAF	Department of Water Affairs
EC	Electrical Conductivity
FA	Factor Analysis
GMWL	Global Meteoric Water line
IBE	Ion Balance Error
ORP	Oxidation Reduction Potential
PCA	Principal Component Analysis
PHREEQC	PH Redox Equilibrium in C language
PMWL	Pretoria Meteoric Water Line
RBplat	Royal Bafokeng Platinum Mine
SAR	Sodium Adsorption Ratio
SSPS	Statistical Package for Social Sciences
TDS	Total Dissolved Solids
TSF	Tailings Storage Facilities
WHO	World Health Organisation
WISH	Windows Interpretation Software for hydrogeologists

MINING TERMS

ANFEX/ANFO	An explosive mixture of ammonium nitrate and oil. Used for blasting underground.
Hanging wall	The rock/roof wall above a mining excavation.
Haulage	An underground excavation that is developed as a hallway for all the relevant services such as water and electricity to get to the ore-bearing excavations.
Merensky Reef	A chrome layer that is loaded in platinum group elements; it occurs in the upper critical zone of the Rustenburg layered suit.
Raise line	Mining excavation used as primary development.
Roof bolt	A long steel bolt that is inserted into the roof of an underground excavation to strengthen the pinning of the rock strata
Sidewall	The rock or wall on the side of a mining excavation.
Stopes	Ore-bearing excavation where blasting of the actual commodity takes place

CHAPTER 1
INTRODUCTION

1.1 Background

From prehistoric ages to the 1900s, the ultimate objective of groundwater studies was to explore and nurture groundwater resources (Fitts, 2013). After the passage of countless eras, the objective remains unchanged. The science of groundwater has become increasingly significant with the enormous increase in population and this has led to the involvement of additional branches such as geology, engineering, and chemistry (Fitts, 2013).

Due to high concentrations of potent and unnatural chemicals, the mining industry is unreservedly linked to pollution of the natural environment, which has effects that remain for decades after mining (Sumi et al., 2001; Kitula, 2005; Khan et al., 2016). The quantity and quality of water resources are compromised daily by mining activities (Khan et al., 2016). Aquifers in mining areas, farms and villages are exposed to a variety of disturbances. These disturbances include domestic use, farming and mining activities or even natural geochemical processes such as water-rock interaction (Ligavha-Mbelengwa, 2017).

North Shaft of RBplat has had challenges with some of the ventilation fans because of groundwater seepage. Ventilation fans that are drawing air from the surface to underground are also drawing groundwater and therefore, flooding takes place in the underground areas and on the surface where the fans are situated. The fans are also rusting due to the moisture that is being drawn in. Another major and common issue which is caused by water in RBplat is surface boreholes which were previously drilled for reef exploration. Underground areas which are mining around surface boreholes tend to be water zones where the hole serves as a conduit and transports water either from the surface of the aquifer into the underground workings.

To curb the impact of mining activities on groundwater resources, a thorough understanding of the processes that compromise groundwater quality is important. Knowing the processes that control groundwater evolution will provide a better understanding of the hydrogeochemical characteristics of an aquifer (Elanqo and Kannan, 2007).

Numerous, extensive studies relating to hydrogeological characteristics and processes in the mining environment have been conducted, particularly concerning acid mine drainage. Unlike gold mining, in the platinum mining industry, multiple reports on groundwater have been

produced by consulting companies, but very few studies were conducted on the hydrogeological characteristics and processes of groundwater in the Royal Bafokeng Platinum Mines. With the goal of exploration of groundwater, this study aims, through various applications, to investigate the hydrogeological processes, evolution, and characteristics of groundwater at Royal Bafokeng Platinum Mines (RBplat), which are found in the western limb of the Bushveld Igneous Complex (BIC) (Figure 1.1).

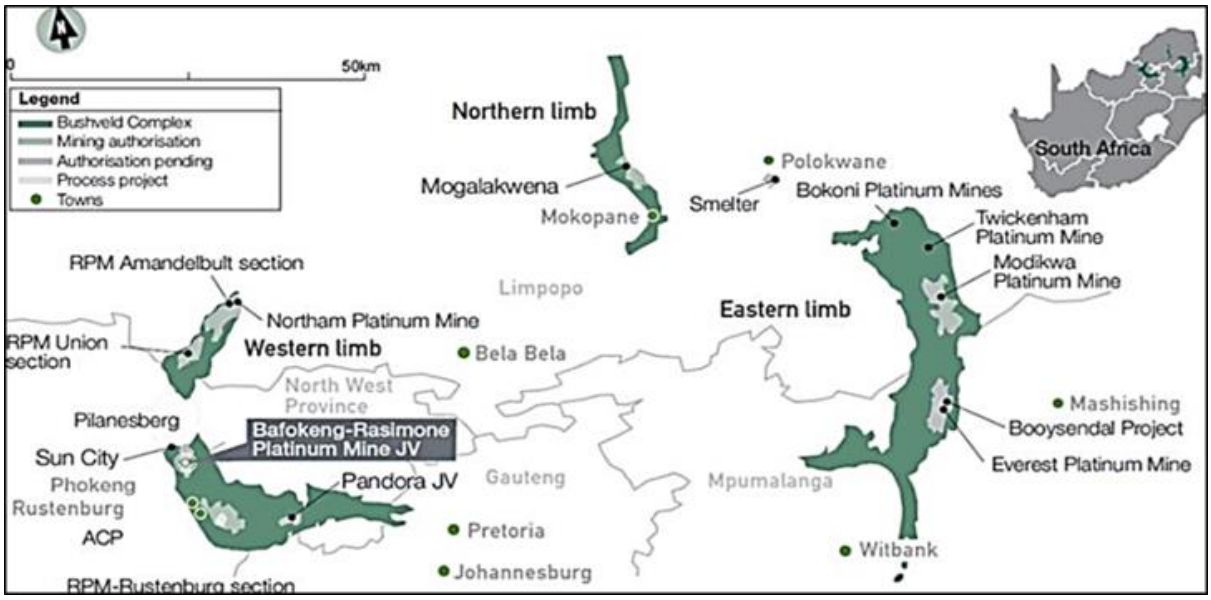

Figure 1.1: Royal Bafokeng Platinum Mine (Source: Padiachy, 2015).

Investigation of hydrochemical processes of groundwater requires an accurate and detailed analysis of the groundwater chemistry. In this study, multiple geochemical tools, such as inverse geochemical modelling, stoichiometry and isotopic ratios have been used to determine the hydrogeochemical characteristics of groundwater in the western limb of the BIC. The elevated rate of mineral exploration taking place in the area was taken into consideration.

1.2 Aims

- Investigate hydrogeochemical characteristics and processes of the groundwater at RBplat in the western limb of the BIC.

1.3 Specific objectives

- Collect hydrogeochemical data, including water samples from underground workings within RBplat.

- Investigate the hydrogeochemical evolution of groundwater using geochemical modelling.

- Use stoichiometry to determine the behaviour of anions and cations in the groundwater system.

- Assess groundwater quality and compare findings from hydrogeochemical characteristic to those in nearby mines.

  Deduce the source of water ingress into underground workings at North Shaft (RBplat).

1.4 Limitations of the study

The major limitation of this study was the use of pre-existing data that was collected many years ago. The use of pre-existing data can be a limitation if there is no proof of the authenticity of data sampling and analysis, especially data from many years ago.

Regarding existing literature, no hydrogeochemical study has been conducted in the Royal Bafokeng Platinum Mine (RBplat) using bivariate plot analysis, stoichiometric ratios, saturation indices or stable isotopes. Studies done in the BIC do exist, but very few of this nature concern specifically the RBplat.

CHAPTER 2
LITERATURE REVIEW

The volume of existing literature relevant to the study at hand mainly derives from consulting companies that conducted environmental assessments for mining companies in the BRPM group. Consequently, few papers were published because academic research is linked to a few authors whose names come up very often in literature on the subject of interest. This indicates the necessity for extensive research and investigation of hydrogeochemical processes in the BRPM. In this chapter, pre-existing reports and journals that are relevant to the study will be acknowledged together with their substantiated findings.

The fact that the BIC harbours some of the world's richest ore deposits, makes it attractive to business ventures related to mining. Of all the minerals present in the stratigraphy, it is only the chromite and sulphide group minerals that have mineralisation with economic significance. The chromite and sulphide group minerals contain over 80% of the world's platinum group metals (Cawthorn, 2010). In this study, the western limb groundwater system of the BIC is of interest.

2.1 Aquifer system

A comprehensive aquifer model was revealed by extensive groundwater projects that were carried out in the BIC by various mining companies. The aquifer system in the BIC comprises a weathered zone immediately below the surface. It is a perched aquifer, which is underlain by a bedrock aquifer and is fractured and semi-confined. In the proximity of the mining areas, the aquifer system is partly dewatered for mining operation purposes. In a nutshell, a crystalline rock aquifer regionally consists of two layers of a deeper fractured bedrock aquifer, which is overlain by a shallow weathered aquifer system (Chilton and Foster, 1995).

Hiscock (2005) states that the crystalline aquifers (igneous and metamorphic rock) types have low porosity relative to well-sorted sedimentary rocks. What controls the groundwater flow in crystalline aquifers is secondary porosity, which is mainly fracturing in the form of faults and joints.

Illustrated in figure 2.1 is a profile that classifies the two aquifer layers that are said to exist in crystalline rock aquifers with their relative physical properties. The perched aquifer, which is semi-confined and immediately underlying the Earth’s surface, is part of the regolith, which

was formed because of the in situ disintegration of underlying noritic rocks (Chilton and Foster, 1995).

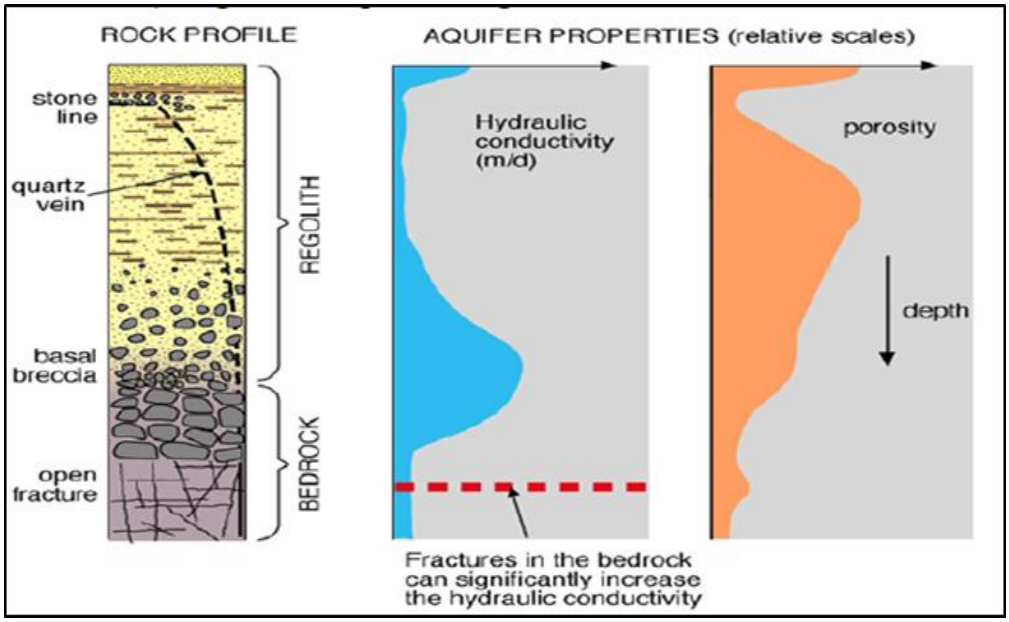

Figure 2.1: Rock profile versus aquifer properties of the crystalline rock aquifer (Source: Chilton and Foster, 1995).

2.1.1 Groundwater flow

Patterns of groundwater flow in an aquifer system are generally influenced by the aquifer material which controls the hydraulic conductivity of an aquifer system. The recharge and discharge rates that are a form of groundwater flow are to some extent controlled by transmissivity. The hydraulic conductivity, which is directly proportional to the transmissivity, usually varies from low to medium and the recorded transmissivity around 18 Shaft of Impala, which is 9 km northeast of Rasimone, was measured at between 0.002 and 0.15 m^2/d (Lenkoe-Magagula, 2013).

A hydrogeological investigation conducted in Marikana (on the other side of the Western BIC), provides evidence that groundwater flow towards the topography is low (Delport, 2012). Figure 2.2 shows the conceptual model on the relationship between groundwater flow and the topography in the Marikana area. The project conducted by Imrie et al. (2014) around the BRPM also observed a durable link between topography and groundwater flow.

Even though there are natural factors that control groundwater flow, many added anthropogenic factors influence the groundwater flow, especially in mining areas such as the BIC. Locally, the groundwater table tends to create a mound around return water dams and tailings storage

facilities owing to activities in the area. However, the water table forms a cone of depression because of water flowing into the mine in the process. Regional groundwater in the demarcated BRPM mine flows from the southwest to the northeast direction (Imrie et al., 2014).

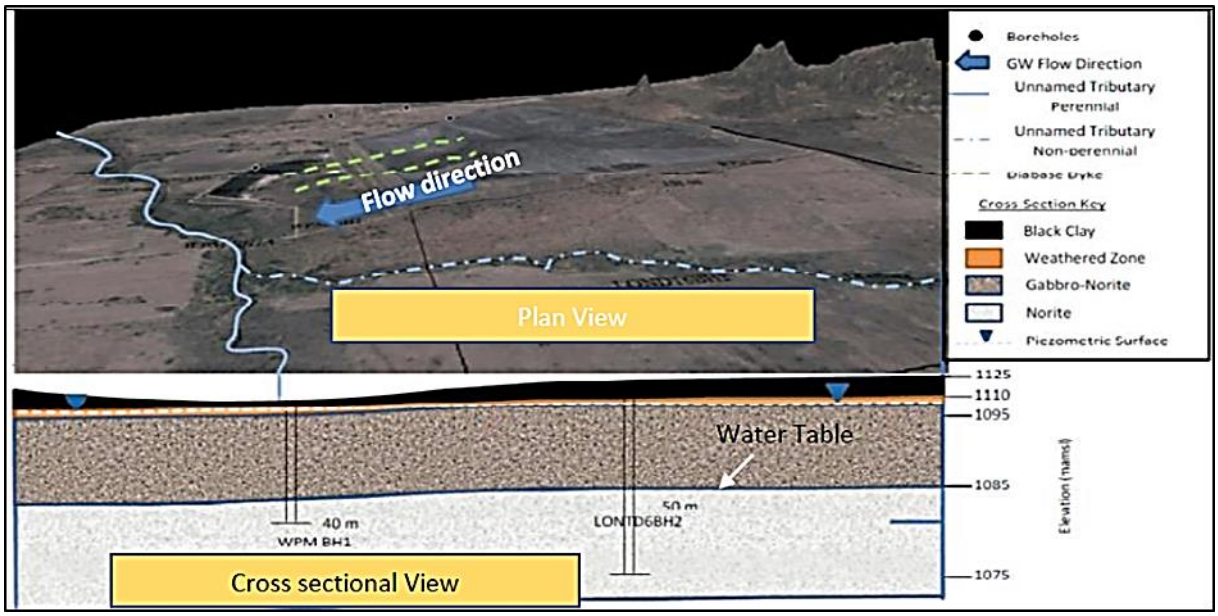

Figure 2.2: Plan and a cross-sectional view illustrating the relationship between topography and groundwater flow (Source: Imrie et al., 2014).

2.1.2 Groundwater levels

The groundwater level which is defined by the height of the water table above sea level is inevitably affected by mining activities. This is so since some mining excavations are well developed below the water table owing to the position of the commodity of interest. Also, before the commencement of mining, companies are forced to dewater the area to develop mining excavations. In other cases, during mining, fractures that are created by mining stress as well as geological structures, allow groundwater circulation into the mining excavations (Das and Karmakar, 2012). These two processes affect groundwater levels in the sense that there is always a manmade depression of the water table due to the reduction in groundwater level. The water level near the mine shaft is always lower than the area away from the mines (Das and Karmakar, 2012).

2.1.3 Hydrogeochemical parameters

Before the commencement of mining in the form of an open-cast mine in the Eastern BIC, Delta H Company was subcontracted to conduct a groundwater assessment in the mining area. Among other groundwater checks, a qualitative study was done by collecting water samples

from different boreholes. The results presented by Delta H for total dissolved solids (TDS) ranged between 464 and 924 mg/l, while pH values were in the range of 7.6 to 8.5 and electrical conductivity (EC) values ranged from 75.6 mS/m to 151 mS/m.

In a different study, a groundwater assessment was conducted in the Western BIC for 18 Shaft of Impala Platinum Mine. The study revealed exorbitant amounts of TDS in the groundwater. Sampling which was conducted in 2010 and 2011 resulted in high TDS values. The highest value recorded in the two years was 10 688 mg/l, with the lowest recorded being 174 mg/l. The pH reading for the groundwater in the area ranged from 6.5 to 8.2 (Lenkoe-Magagula, 2013). The results from both studies which were conducted at the opposite ends of the BIC coincide with each other since neither is within the recommended drinking water limits.

To extend one of the tailings storage facilities at RBplat, the mine subcontracted SRK Consulting to carry out an environmental impact assessment which necessitates the testing of groundwater quality. Samples collected from the community boreholes around the mine indicated that the reported TDS value at the time of the assessment in 2014 had significantly decreased from over 1200 mg/l to below 700 mg/l. According to this report, the high TDS readings from Rasimone boreholes were unlikely given the tailings storage facility (TSF) (This was indicated by low concentrations between TSF and Rasimone boreholes.)

At approximately 50 km northwest of the Frischgewaaged and Boschkoppie farms, Van Coller (2013) conducted a study looking into flooding an open pit as environmental rehabilitation post open pit closure. The study took place around the Pilanesberg Platinum Mines where platinum mining had been taking place for over 16 years. The data collected around the area from groundwater monitoring boreholes indicated TDS ranging between 25 mg/l and 604 mg/l. These values are well below the standard limit of 1200 mg/l. From the same boreholes, the lowest and highest recorded pH values were 7.6 and 9.11 respectively (Van Coller, 2013).

2.1.4 Hydrochemistry

The chemical constituents contained in groundwater are due to multiple processes such as biogeochemical interactions between the groundwater, its host rock and the soils it percolates (Hiscock, 2005). Hiscock (2005) further states that the composition of rainwater around groundwater recharge zones plays a significant role in the ultimate chemical composition of groundwater. In addition to water-rock interaction and rainfall composition, processes such as

seawater and groundwater mixing in coastal areas also influence the final composition of groundwater.

To determine the status quo of the groundwater and identify potential groundwater use, groundwater sampling was conducted using selected boreholes in the eastern limb of the BIC before the commencement of open-cast mining 17 km southwest of Steelpoort (Hollard and Rossouw, 2016). The hydrochemical results revealed arsenic values higher than the World Health Organisation (WHO) standard for drinking water (2011) and exorbitant amounts of TDS at 860 mg/l (max.) and 502 mg/l (min.) compared to the domestic limit of 450 mg/l as determined by the Department of Water Affairs (DWAF, 1996b). Some boreholes had chloride and nitrate values that exceeded the limits. The pH value and other major ions such as calcium, potassium, sulphate were within the recommended limits (Hollard and Rossouw, 2016). Even though its findings were not conclusive, according to the report, the suspected source of elevated nitrate values (between 0.1 mg/l and 29 mg/l) was residues from explosives and other activities related to mining. The chloride concentrations ranged between 128 mg/l and 157 mg/l and were attributed to the combined effect of water-rock interaction and minimal recharge (Hollard and Rossouw, 2016).

Hydrochemical analysis of groundwater sampling conducted around the Pilanesberg platinum mines by Van Collar (2013) found that most of the concentrations were within the set standards. Forty percent of the samples had concentrations of magnesium that were over the limit of 70 mg/l, followed by 30% of samples with fluoride exceeding the set standards of 1.7 mg/l. With a deviation of 20% from the standards, nitrate and iron followed suit. The report concluded that water sources with values exceeding the set limits were not consumable and the high concentration of NO_3 was due to explosives used for blasting (Van Coller, 2013).

Among other ions found within the groundwater of the Western Bushveld, the concentration of fluoride, which is up to 80 mg/l in the Pilanesberg complex, has attracted a lot of attention from hydro-geoscientists. McCaffery (1998) investigated the distribution and causes of high fluoride groundwater in the Western BIC and reported that of over 338 groundwater samples analysed for fluoride, approximately 68 samples had concentrations exceeding 1.5 mg/l. Geochemical analysis of rocks indicated that the Lebowa granites and Pilanesberg Alkaline Complex contain fluorite and apatite that generate fluoride in groundwater.

2.1.5 Water types

Groundwater is classified according to its major ion constituents. The name is, therefore, derived from the dominant ions in a water-based concentration. The shallow weathered aquifers contain Mg-Ca-HCO_3 water type, as displayed by Figure 2.3, which varies to Mg-Ca-HCO_3-Cl closer to alluvial aquifers and along with major river systems such as the Crocodile River. Water facies resulting from the water stored in the deeper fractured aquifers are highly evolved Na-Cl water facies (Chilton and Foster, 1995).

Results from the groundwater impact assessment conducted by SRK consulting on 18 shafts confirm the above-mentioned water types with an indication of Mg-Ca-HCO_3 water facies. The Mg-Ca-HCO_3 water is linked to the chemical weathering of ferromagnesian minerals such as biotite, pyroxenite and olivine, which happen to be the major sources of mineralisation in the BIC (Lenkoe-Magagula, 2013).

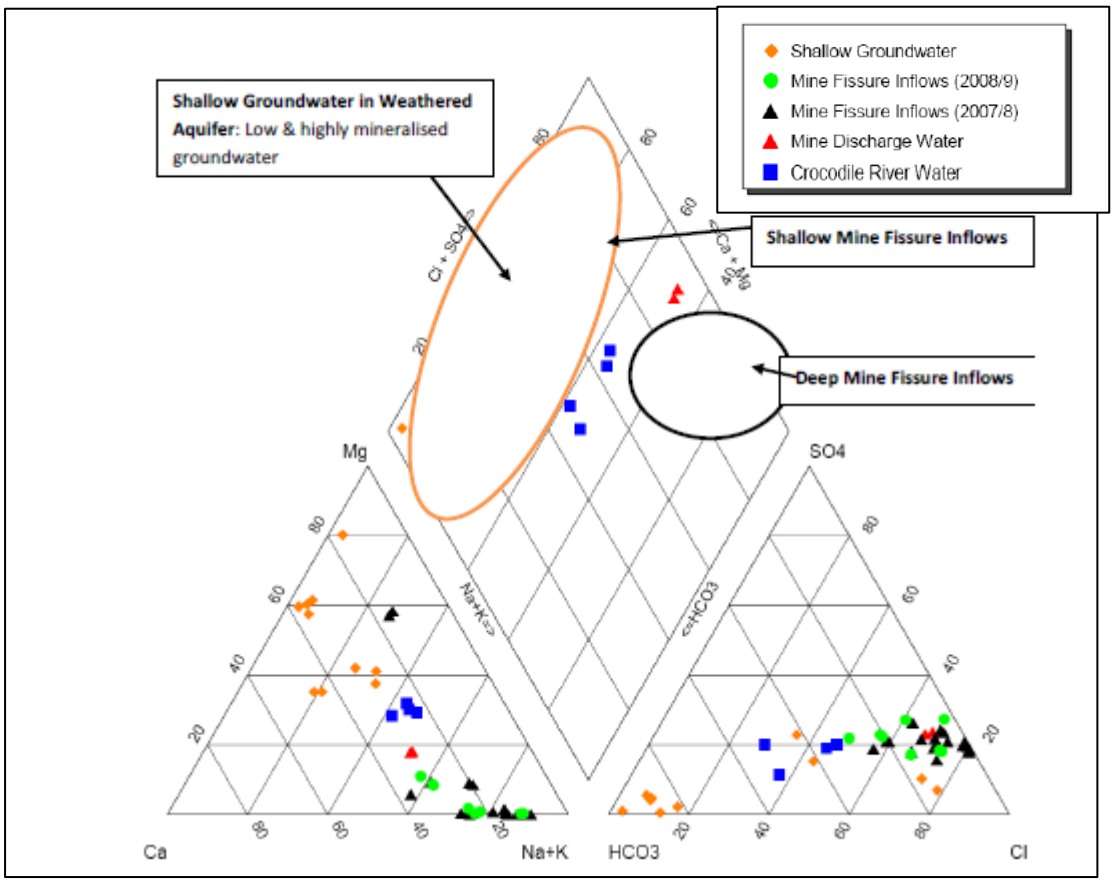

Figure 2.3: Piper plot illustrating common groundwater types found in the crystalline rock aquifers in a mining environment (source: Titus et al, 2009).

2.1.6 Hydrogeochemical processes

According to Hiscock (2005), the hydrochemical makeup of groundwater changes with depth, as bicarbonate water types are dominant at the outcrop and then the water becomes more saline as it goes deeper beneath the Earth's crust. Hiscock (2005) mentions the distinction of water types in the form of hydrogeological facies and attributes this to water-rock interaction, which depends on the hydrogeological environment. Apart from water-rock interaction, many hydrochemical processes influence or change the groundwater chemistry through its pathway. However, depending on the environment, the distribution of ions in the water may change owing to ions being leached, reduced or precipitated. In other cases, the ions are exchanged (Hiscock, 2005).

A hydrogeochemical study conducted in the eastern limb of the BIC (30 km northwest of Mokopane town) by Atangana et al. (2017) indicated the mixed water type as the most dominant, followed by the Mg-HCO_3 water type. There were questions on the mixing processes between freshly recharged water and contamination as the cause of the non-dominant water type. This was based on the suggestion that if there is no dominant water type, then there is a mix of different water types. The magnesium-bicarbonate water type is linked to the mafic and dolomitic rocks of the BIC and the Transvaal Supergroup because they are rich in calcium, magnesium, and bicarbonate. This suggests processes of interaction between the host rock and groundwater (Atangana et al., 2017).

From a groundwater assessment conducted in the Western BIC, the Mg-Ca-HCO_3 water type was attributed to the weathering of ferromagnesian and silicate minerals which are constituents of feldspar minerals commonly found in the BIC (Lenkoe-Magagula, 2013). Lenkoe-Magagula (2013) further suggests that even though the water type could result from the weathering of dolomitic rock types, the calcium-to-magnesium ratio, in this case, is indicative of ferromagnesian and silicate weathering.

CHAPTER 3
STUDY AREA

The crystalline aquifer of the BIC, which is the target of the study, is situated approximately 30 km to the northwest of Rustenburg (Figure 3.1). This aquifer system is positioned beneath the RBplat farms in the Boschkoppie 104 JQ and Frischgewaaged 96 JQ, with the surrounding villages such as Mafenya, Robega, Chaneng, and Rasimone. Mining activities are currently taking place in three shafts: North, South, and Styldrift I (Padiyache, 2015). The three shafts extract platinum group elements from the well-known Merensky and Upper Group 2 Reef. The dip of the orebody hosting these Reefs is between 9 and 15 degrees, allowing both open-pit and underground mining activities. The North and South Shafts, developed immediately adjacent to the mined-out open pits, are decline shafts, while Styldrift 1 is vertical. All these shafts have intersected groundwater during development. In some areas, such as in the declines, intersected groundwater can be observed. This water is observed as water drops dripping from the hanging wall and the sidewall.

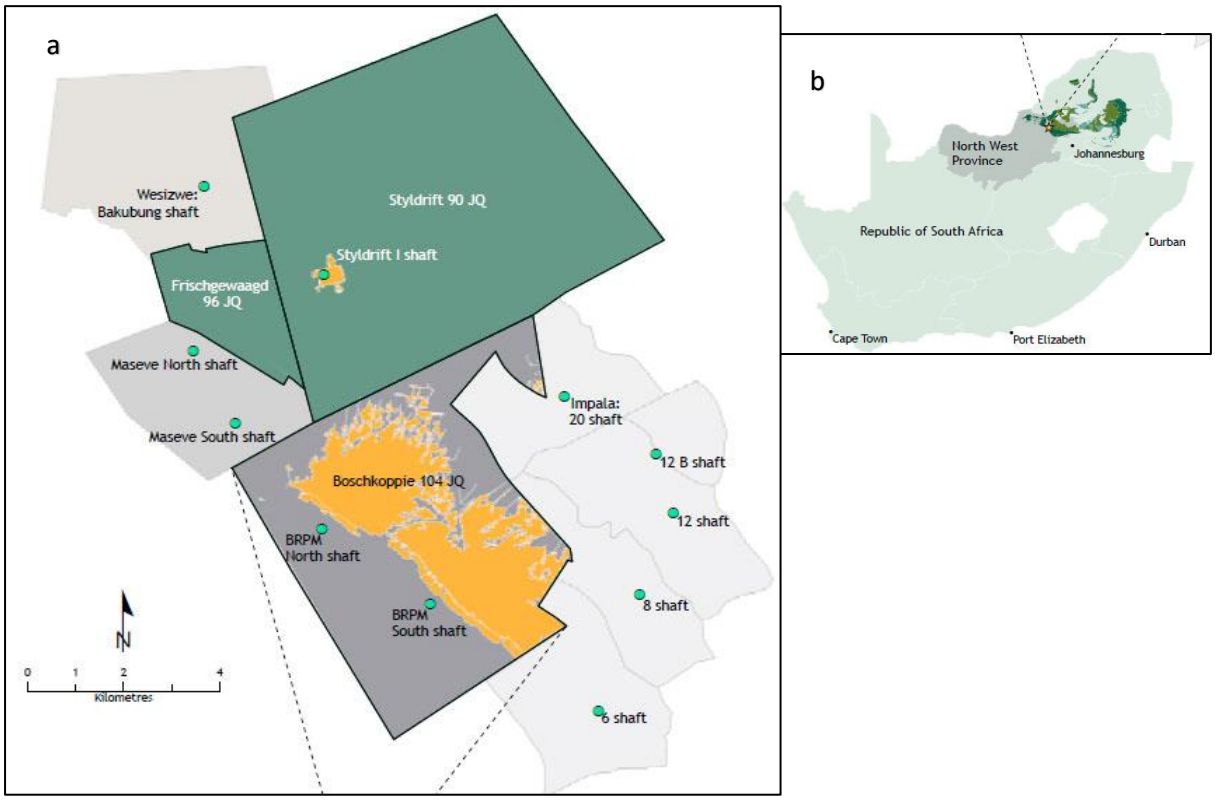

Figure 3.1: (a) Map showing the study area. (b) Insert; South Africa showing the study area (source: http://www.bafokengplatinum.co.za/brpm-joint-venture.php).

3.1 Geological setting

The Bushveld Igneous Complex is a mafic layered intrusion with an extensive granitic mass, which dates to the Paleoproterozoic era where it was emplaced on the Kaapvaal Craton (Kinnard et al., 2005; Friedman, 2008). The complex is an intrusion that intruded the Transvaal Supergroup and Pretoria Group rocks (Kinnard et al, 2005; Friedman, 2008). Among other layers, the BIC comprises the Rustenburg Layered Suite which has an area of 65000 km^2 and a depth of approximately 8 km (Cawthorn et al., 2006) and is divided into four exposed limbs and a fifth covered by younger sediments. The exposed limbs are the Northern, Eastern, Western and Far Western Limb (Kinnaird, 2016). The limbs are named based on their location and occurrence in the Mpumalanga, North West and Limpopo provinces of South Africa.

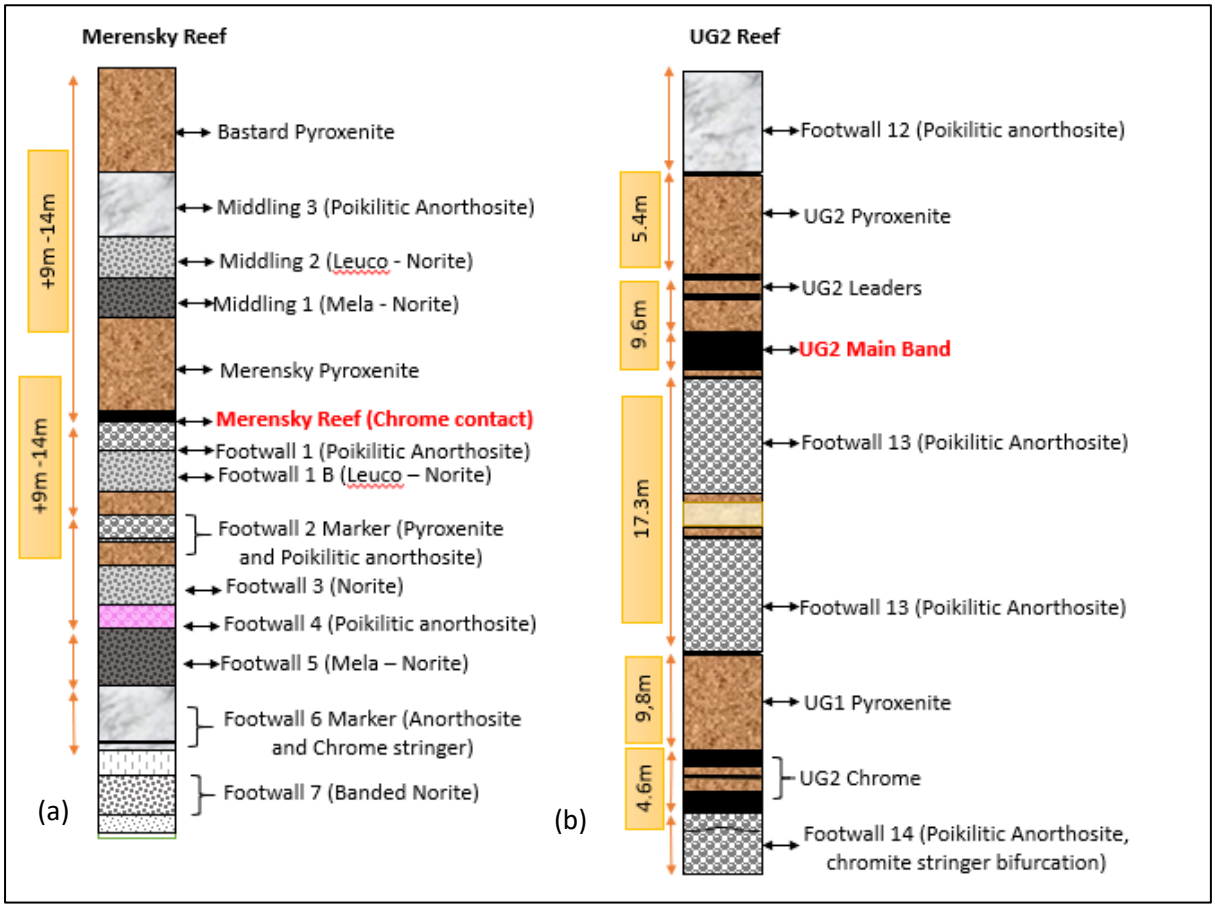

Figure 3.2: (a) Stratigraphic column of RBplat showing the Merensky Reef section. (b) Stratigraphic column of RBplat showing the UG2 Reef section (Source: RBplat, 2015).

Out of all the minerals present in these layers, it is only the chromite and sulphide group minerals that have mineralisation with significant economic value. The chromite and sulphide group minerals have over 80% of the world's platinum group metals (Cawthorn, 2010).

Figure 3.2 shows the stratigraphic column of Royal Bafokeng Platinum Mine, constructed from the core logging, which was conducted during the mineral exploration in the area. The stratigraphy is continuously modified from underground mappings. RBplat is mining the Merensky reef and the UG2 reef types. The two reef types are 70 m apart with the Merensky reef type above the UG2. The two-reef types as seen on the stratigraphy are bounded by alternating layers of pyroxenite, anorthosite and norite. An XRD analysis was not performed for this project but from general knowledge of rocks in the area and existing literature of local geology, the study area comprises primarily of silicates followed by sulphide minerals.

The Royal Bafokeng Platinum Mine stratigraphy is generally disturbed by dolerite intrusions (dykes and sills) and IRUP (Partial and Complete). The dolerite intrusions are sheet-like bodies that form within fractures in the area. The intrusions have fine to medium crystal size and they appear to be dark green to grey (mafic minerals). Iron-rich ultramafic pegmatites (IRUP) appear in a form of veins or irregular patches. These IRUPs have large interlocking crystals which are usually black with minimal felsic minerals appearing. The complete IRUP replaces the reef stratigraphy while with the partial IRUP the reef stratigraphy can be observed and recovered. Both dolerite intrusions and IRUP can negatively affect the mining process depending on their orientation and size (Villers du Preez, 2018). In terms of size, the bigger the structure the severe the effects on mining. Dolerite tends to be more disruptive to mining when it is in a form of a sill (0° to 45°) and IRUP tends to be destructive when it completely replaces the reef (Villers du Preez, 2018).

Table 3.1 and Table 3.2 show the silicate mineral groups that are found within the Bushveld Igneous Complex with examples and chemical formulas (Schouwstra et al., 2000). Knowledge of minerals and their abundance will assist in giving possible origins of water based on the rocks that the water interacts with as it flows.

Table 3.1: Primary silicates which occur in the Bushveld Igneous Complex together with their abundance and chemical formula (Source: Schouwstra et al., 2000).

Mineral Group	Abundance	Mineral Example	Formula
Pyroxenes	Major	Enstatite	$MgSiO_3$
		Bronzite	$(Mg, Fe^{2+})_2 (SiO_3)_2$
		Augite	$(Ca, Na)(Mg, Fe^{2+}, AlFe^{3+}, Ti)[(Si,Al)_2O_2]$
Feldspar	Major	Anorthite	$CaAl_2Si_2O_8$
		Labradorite	$(Ca, Na)[Al(Al,Si)Si_2O_8]$
		Andesite	$(Na, Ca)[Al(Si,Al)Si_2O_8]$

Olivine	Major	Forsterite	Mg_2SiO_4
		Fayalite	Fe_2SiO_4

Table 3.2: Secondary sillicates which occur in the Bushveld Igneous Complex with their abundance and chemical formula (Source: Schouwstra et al., 2000).

Mineral Group	Abundance	Mineral Example	Formula
Amphibole	Minor	Magnesiohornblende	$(Ca_2)(Mg_4Al)(AlSi_7O_{22})(OH)_2$
		Riebeckite	$(Na_2)(Fe_3^{2+},Fe_2^{3+})Si_8O_22(OH)_2$
Micas	Minor - trace	Annite	$KFe_3^{2+}(AlSiO_{10})(OH)_2$
		Phlogophite	$KMg_3(AlSi_3O_{10})(OH, F)_2$
Chlorite	Minor - trace	Clinochlore	$(Mg. Fe^{2+})_5Al(AlSi_3O_{10})(OH)_8$
Clay	Minor - trace	Talc	$Mg_3(Si_4O_{10})(OH)_2$
Serpentine	Minor	Antigorite	$(Mg, Fe^{2+})_3(Si_2O_5)(OH)_4$
		Dickite	$Al_2(Si_2O_5)(OH)_4$

3.2 Hydrogeological outline

The most important geological features in the hydrogeology of an area are geological discontinuities such as dykes, faults and fractures (Gupta and Singhal, 2010). Most discontinuities such as dykes and faults are storage facilities and conduits that control the groundwater flow. In fractured aquifers, joints, faults and shear zones are the main water channels. Understanding the hydraulic characteristics of these rocks helps in understanding the movement of groundwater (Gupta and Singhal, 2010). Table 3.5 presents common geological structures around RBplat along with their mineral content.

Table 3.3: Geological structures that occur around RBplat with their mineral content.

Geological Structures	Mineral Content
Dolerite	Plagioclase, Pyroxene
Lamprophyre	Feldspar, pyroxene, Amphibole, sulphides, fluorite, biotite
Pegmatite veins	Plagioclase feldspar (albite and anorthite), mica

The water levels, as observed in the water-monitoring boreholes in the area, vary from 3 m to 30 m below the ground surface. The groundwater level at South Shaft reads at an average of 21 m below the surface, while the average water level at the North Shaft is 10 m. The groundwater level is at 20 m below the ground surface around Styldrift I.

Figure 3.3 is an illustration of a cross-sectional view of RBplat created from two exploration boreholes and groundwater monitoring data. The groundwater level ranges from 3 m to 30 m

below the surface indicating that this could be a shallow aquifer. The area has an overburden with an average thickness of 3.6 m and the weathered zone with an average thickness ranging between 9 m and 21 m. The weathered zone is mostly pyroxenite and talc in other areas. At the depth approximately below the weathered zone, the rock type is a norite, which is fractured by faults and interconnected joints.

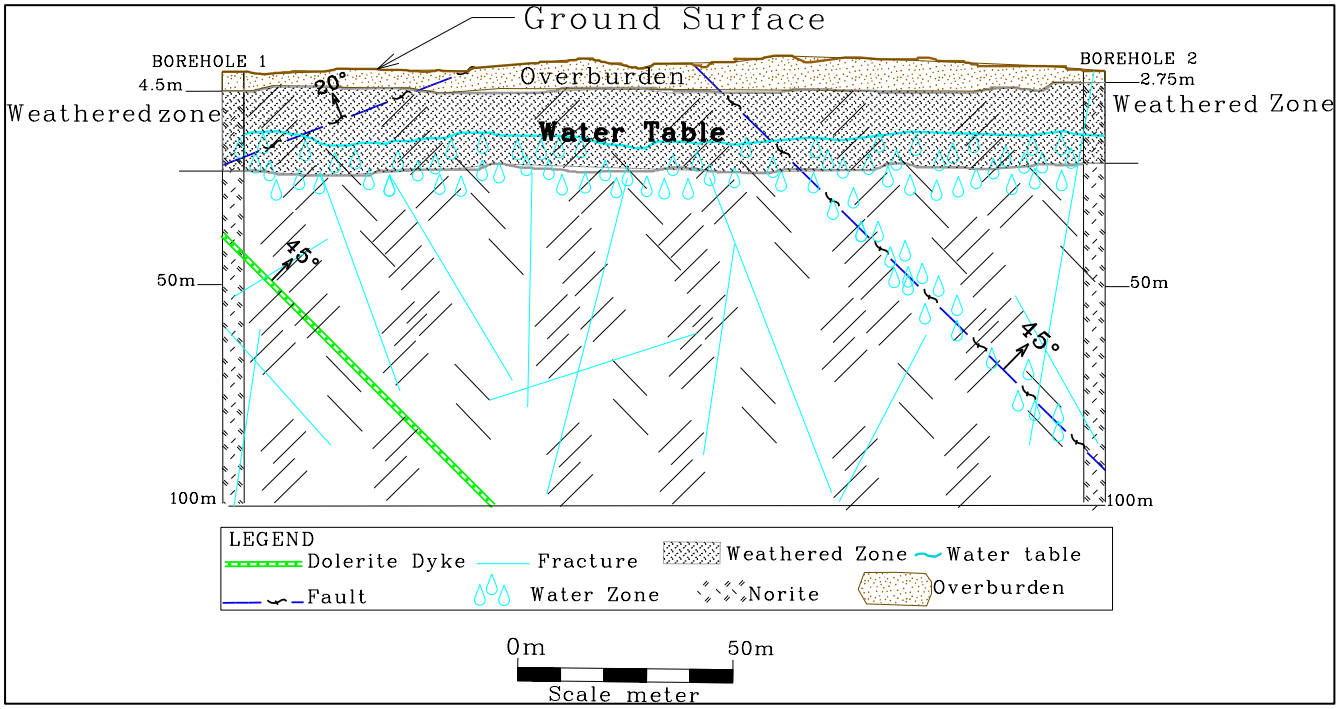

Figure 3.3: Cross-sectional view of RBplat showing the Groundwater level in relation to the ground surface and the weathered zone. The section was created from the borehole loggings as well as information derived from the groundwater monitoring boreholes.

Images of different fractures that exist around the mine are shown in Figure 3.6. In the mining environment, there are different types of fractures, some are natural fractures and others are stress-induced fractures. Stress-induced fractures are fractures that exist from mining activities such as blasting, and unlike natural geological fractures, they are young, not continuous and they are not mostly infilled. There are also localized fractures and regional fractures. In RBplat, localized fractures tend to have minimal impact on the ground condition and have limited or no water flow. Regional fractures usually have a significant impact on the ground condition because generally, they have high and consistent water flow and extend over kilometres, both laterally and vertically.

The fracture aperture in the area ranges between 0 mm to 10 mm collected from underground mappings and core logging. While some fractures are infilled, others are not infilled. From

optical inspection, fractures in the RBplat area are usually infilled with chlorite, calcite, or serpentinized minerals.

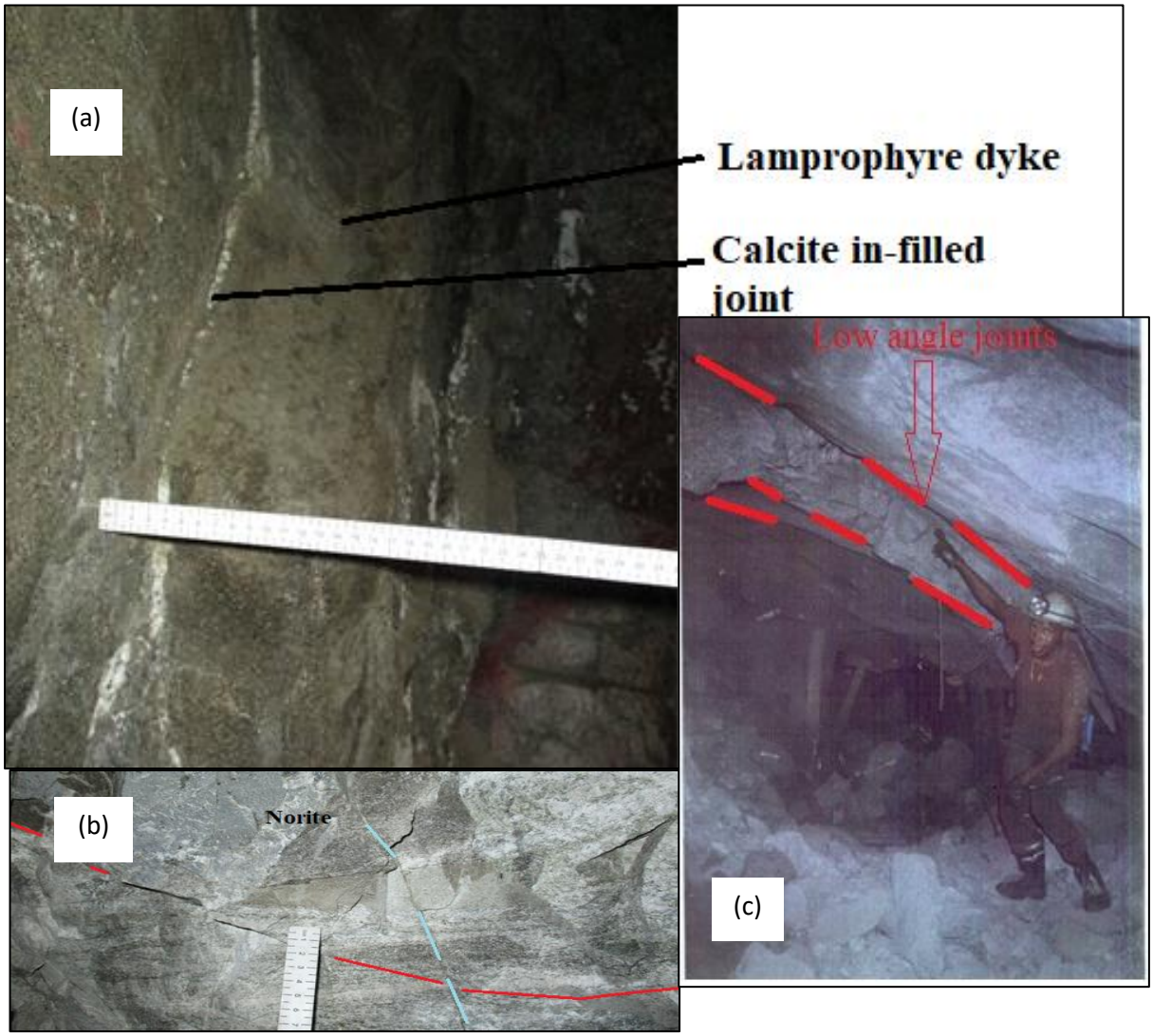

Figure 3.4: Fractures commonly found in the RBplat area (a) A joint that has a thick white infilling. (b) A fractured norite with a Subvertical joint (turquoise) and a low angled joint (red) (c) A picture of a prominent low angle joint with a large opening.

3.3 Hydrological outline

The Elands River is the largest and longest watercourse that flows through the vicinity of the RBplat (Figure 3.5). The general river flow is from the west to the eastern side of the mine and south of the Pilanesberg. Relative to the three shafts, the Elands River flows on the northern side and South Shaft is the furthest from the river at 8 km. Styldrift I is the closest shaft to the Elands River, with only a kilometre distance to the river channel. This river receives small tributaries such as the Bonwakgobo, Majapele and Matlopyane streams, which carry water

closer to the shafts. Due to variations in their proximity to the river channel, the effect of the river on the shafts varies from one shaft to the other.

Numerous boreholes have been drilled around the farm for different investigative reasons such as geology, hydrogeology and the geochemistry of the area. Some of these boreholes reach to a depth of over 1000 m. They are a significant part of the hydrogeology of the area, as they often act as water conduits to underground workings.

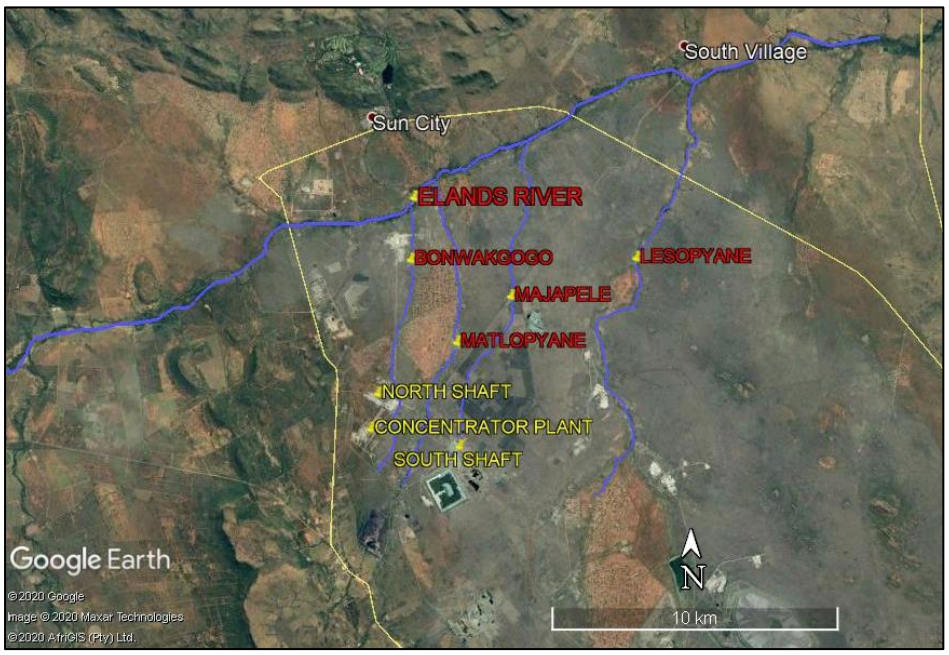

Figure 3.5: Arial Google Earth image illustrating the Elands River and its connected streams flowing around Royal Bafokeng Platinum Mine (Google Earth).

3.4 Climate

The temperature of Rasimone ranges between a maximum of 24.1°C in January, with the lowest temperature of 11.9°C in July (Table 3.1 and Figure 3.2). According to the Koppen-Geiger climate classification, the climate that prevails in Rasimone village is classified as BSh climate (hot semi-arid).

Table 3.4: Monthly temperatures around Rasimone village; average, minimum and maximum in degrees Celsius (2019).

Temp	Jan	Feb	Mar	Apr	May	Jun	Jul	Aug	Sep	Oct	Nov	Dec
Av	24.1	23.3	21.9	18.7	15	12	11.9	14.7	18.9	21.9	22.7	23.8
Min	17.5	16.9	15.3	11.4	6.7	3.2	2.9	5.6	10.2	14	15.6	16.9
Max	30.8	29.8	28.5	26	23.4	20.8	21	23.9	27.6	29.9	29.9	30.7

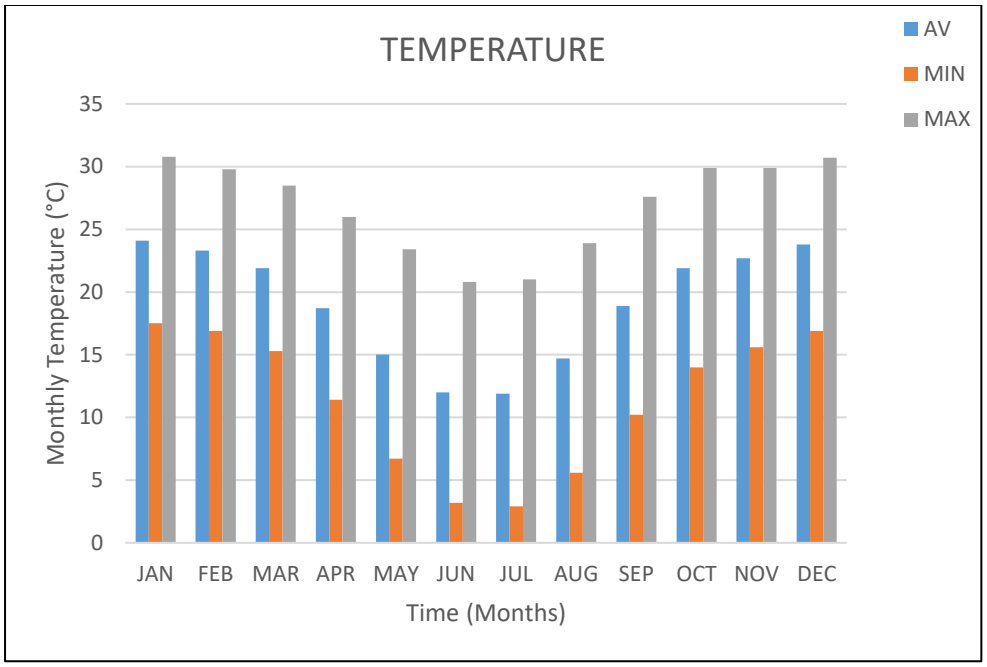

Figure 3.6 Monthly temperatures at Rasimone.

Rasimone has an average rainfall of 113 mm/yr. The area is characterised by minimal to no rainfall in winter and wet summer days. July is the driest month of all, with an average rainfall of 4 mm, while the highest rainfall is recorded in December (Climate data.org 2019); refer to Table 3.5 and Figure 3.7.

Table 3.5: Monthly precipitation (mm) in the Rasimone village (2019).

	Jan	Feb	Mar	Apr	May	Jun	Jul	Aug	Sep	Oct	Nov	Dec
Precip (mm)	**106**	**100**	**96**	**44**	**12**	**9**	**4**	**4**	**17**	**54**	**76**	**117**

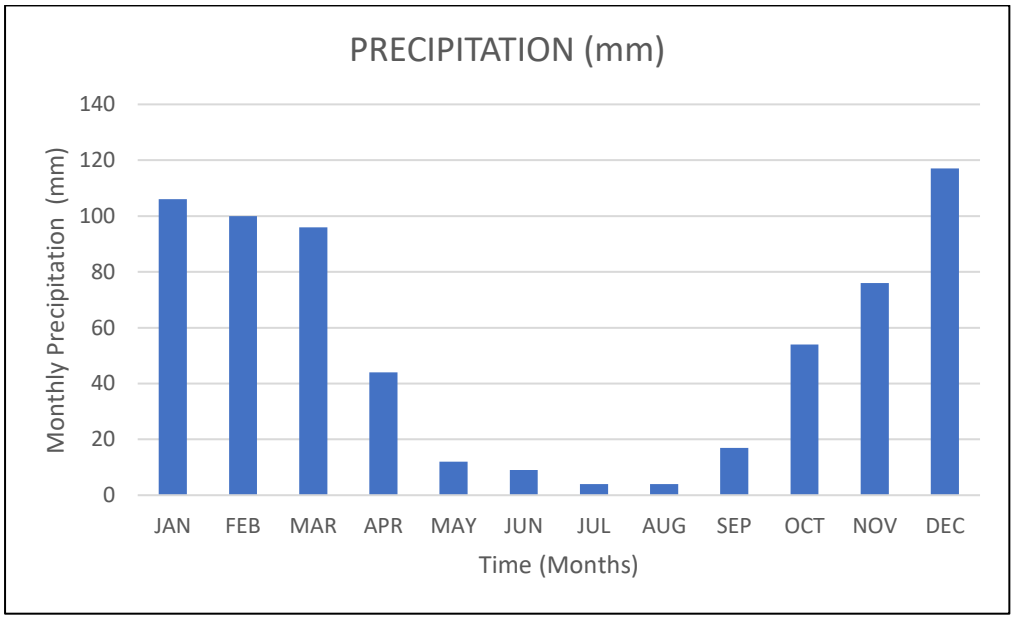

Figure 3.7 Monthly precipitation at Rasimone.

CHAPTER 4
METHODOLOGY

4.1 Desktop study

As previously mentioned, the mine started its operations in 1997 and hydrogeological contractors were outsourced to conduct the water-monitoring activities quarterly just after it had started operating. The purpose of conducting a desktop study was to collect all information submitted by various consulting companies. The information was recorded in the form of reports, data, images, maps and a thorough study of what had previously been reported and conducted. Publications containing data and information relevant to the study were meticulously studied.

4.2 Method and materials

Shortly after the commencement of mining, over 75 boreholes were randomly placed around RBplat, which were selected by the RBplat environmental department for groundwater quality and level monitoring. Initially, the groundwater was only tested for TDS and fluoride. From 2007 onwards, the monitoring procedure was upgraded with multiple parameters such as pH, water levels, major ions and trace elements. The monitoring activity was conducted four times annually. In later years, some boreholes were either demolished or discontinued for several reasons, such as construction and development. The number of monitoring boreholes was further reduced when some became blocked or obstructed, making them impossible to sample.

The monitoring procedure for groundwater assessment purposes was conducted by various hydrogeology consulting companies, which were subcontracted by the mine. The data collected has since been submitted to RBplat for recording in the mine's database.

4.3 Sampling

For this project, only boreholes with complete and consistent data were used from the existing database, which reduced the total number of boreholes to 28, and the data were used to investigate hydrogeochemical processes altering the evolution of groundwater in the area. Sampling was done at North Shaft in March 2019. Mining areas that were targeted were disrupted by water ingress. The samples were taken for metals and major ion analyses to determine the primary water source and water quality.

To validate the pre-existing data, new data were compared with the existing data, while the same methods of investigation were used to determine the evolution and hydrogeochemical processes of the groundwater in the area.

4.3.1 Underground sampling

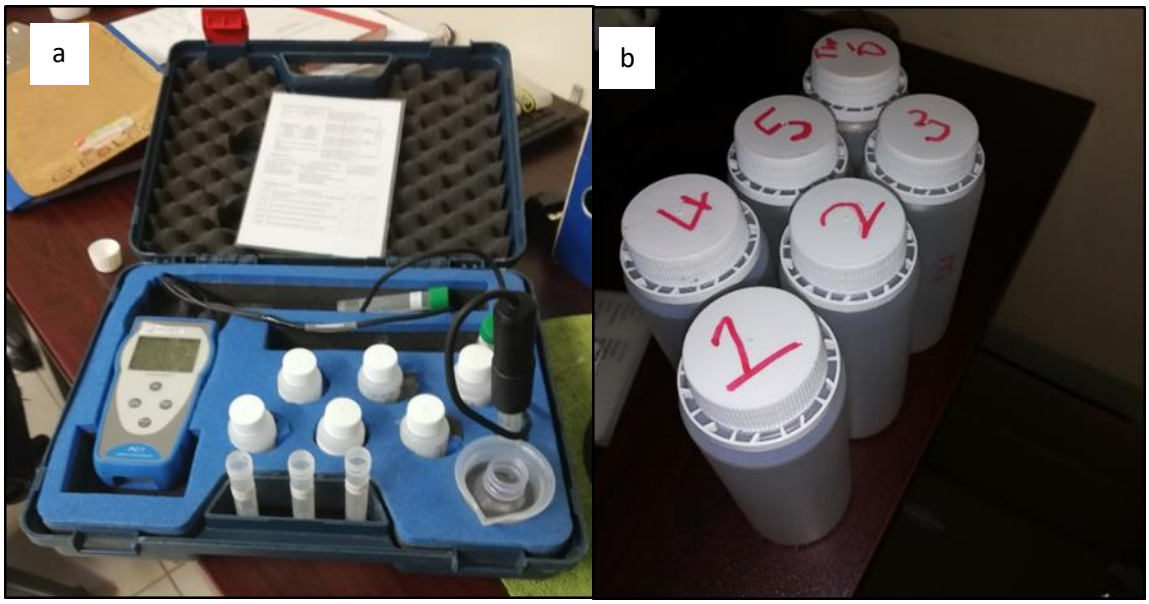

Figure 4.1: (a) A portable multimeter which measures the EC and temperature. (b) Water samples collected from North Shaft.

In addition to the pre-existing data, six water samples were collected from underground at North Shaft in March 2019 (Figure 4.1 a & b). In the latest sampling, some of the samples were directly taken from g fractures where water was seeping into underground workplaces. At each sampling site, a comprehensive hydrogeological inspection of the site was done. Any information that would be valuable in the analyses was noted. This included taking the rate of flow of water and identifying the type of geological structures, as well as the rock type that the structure was cross-cutting.

During sample collection, temperature, EC and the flow rate of water were measured at the site. The EC and temperature were measured using a portable multimeter (Model IACCPC7); 250 ml polyethylene bottles were used to collect water samples, and a few drops of nitric acid were added to the sample to reduce the pH to <2 for preservation purposes. The samples were then stored in a cool, dark place before being taken to the laboratory for chemical analyses.

4.4 Laboratory analysis

The chemical analyses of major ions and metals were done at the Setpoint laboratories. Inductively coupled plasma optical emission spectrometry was used for the following elements: K, Fe, Zn, Mn, Cu, Mg, Ca, As, Al, Na and the automated photometric analyser was used for Cl, F, and SO_4^{2-} . Total alkalinity was determined through the titration method with HCl. Inductively coupled plasma mass spectrometry was used for the analyses of Hg and Pb. Stable isotope data were measured at the Hydrogeology laboratory, School of Geosciences, Wits University.

4.5 Quality and reliability analysis

It was important to conduct a data reliability check to avoid defective results that would be used to make certain decisions. The two methods used to validate the data were cation-anion balance technique (Equation 4.1) and the box and whisker technique (Hounslow, 2018). The ion balance technique makes use of the principle of electroneutrality, which assumes the sum of cations to be equal to the sum of anions. The following equation is used:

$$\boldsymbol{Ion\ Balance\ Error} = \left(\frac{\sum \boldsymbol{cations}\ (\frac{\boldsymbol{meq}}{\boldsymbol{l}}) - \sum \boldsymbol{anions}(\frac{\boldsymbol{meq}}{\boldsymbol{l}})}{\sum \boldsymbol{cations}(\frac{\boldsymbol{meq}}{\boldsymbol{l}}) + \sum \boldsymbol{anions}\ (\frac{\boldsymbol{meq}}{\boldsymbol{l}})}\right) * \mathbf{100} \qquad (4.1)$$

If the calculated ion balance percentage is higher than 11.5%, the data quality is regarded as poor. Box and whisker plots summarise and indicate outliers in a data set (Figure 4.2). High standard deviation/high spread of data is an indication of low precision and extreme outliers are often indicative of errors (Hounslow, 2018).

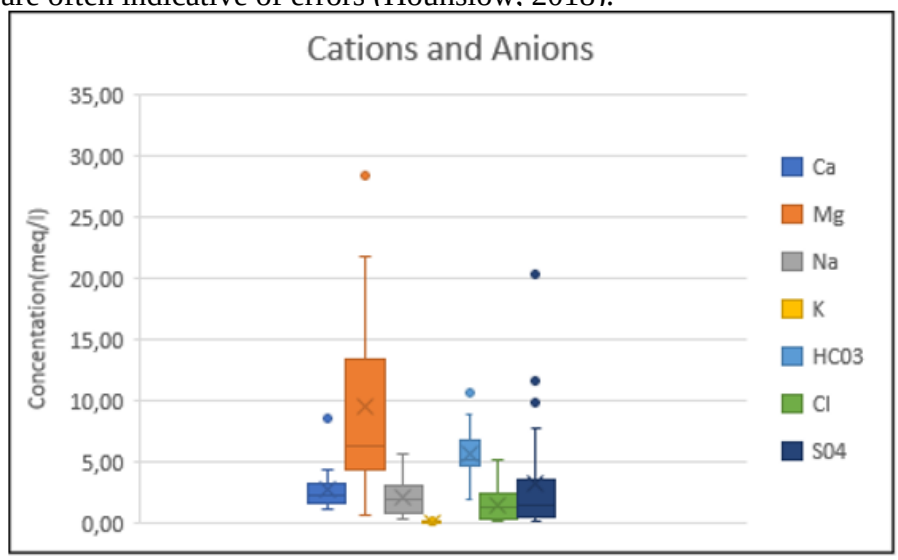

Figure 4.2: box and whisker plots of major ions.

4.6 Bivariate plots

Bivariate plot analysis is a statistical tool that is used to determine the relationship amongst two variables. The correlation plots can be plotted on a Microsoft Excel spreadsheet which will show a trend line and correlation coefficient value. The trend line obtained is used to determine possible hydrogeochemical processes taking place in the aquifer system. A correlation coefficient is usually a number between 0 and 1 (Brown, 2012).

The correlation coefficients will be classified as per Guildford's rule of thumb (Gildford, 1973). The classification is as follows, 0-0.29 is negligible, 0.3-0.49 low correlation, 0.5-0.69 moderate correlation, 0.7-0.89 good correlation and 0.9 -1 best correlation (Kura et al. 2013).

4.7 Mineral saturation indices

PHREEQC interactive was used to calculate the saturation indices of the mineral content in the groundwater data collected around the study area. The saturation indices calculations are used to determine the saturation state of minerals in the water. According to Appelo and Postma (2005), SI = 0 means the mineral is in equilibrium, SI<0 means undersaturation of the mineral which is dissolution and SI>1 is oversaturation which means mineral precipitation. The SI results are presented in Table 5.5.

4.8 Water-rock interaction

To determine some of the processes that contribute to the change of water chemistry, stoichiometric analysis was conducted using the concentration of major ions. The ion concentrations were converted from mg/l to meq/l and molar concentration ratios are calculated.

The following ratio equations are provided by Hounslow (1995) where concentrations were substituted, and results were used to make deductions about the hydrogeological processes affecting certain areas in the system. The possible occurrence of halite dissolution was investigated using equation 2.1. A molar ratio of 1 indicates the dissolution of halite as the prime process contributing to sodium and chloride ions in the water (Jalali, 2009). A molar ratio >1 indicates silicate weathering and <1 indicates ion exchange (Jalali, 2009).

$$r = \frac{Na^+}{Cl^-} \qquad (2.1)$$

Equation 2.2 was used to investigate gypsum dissolution. A ratio that is equal to 1 confirms the dissolution of gypsum as a hydrogeochemical process contributing to the calcium and sulphate ions in the water (Hounslow, 1995). A ratio >0.5 indicates other sources of calcium such as weathering carbonates or silicates while r<0.5 and a neutral pH may indicate the removal of calcium through ion exchange or calcite precipitation (Hounslow, 1995).

$$r = \frac{Ca^{2+}}{Ca^{2+} + SO_4^{2-}} \quad (2.2)$$

A ratio of Ca+Mg/HCO_3 that is less than 1 indicates recent recharge, freshwater recharge or meteoric groundwater (Nazzal et al., 2014; Zaidi et al., 2015).

$$r = \frac{Ca^{2+} + Mg^{2+}}{HCO_3^-} \quad (2.3)$$

According to Hounslow (1995), if molar ratios calculated for silicates using equation 2.4 are <0.2 and >0.8 it is less likely for silicate weathering to take place and when the ratio is 0.2 and 0.8 silicate weathering can be considered in contributing to the groundwater chemistry.

$$r = \frac{Na^+ + K^+ - Cl^-}{Na^+ + K^+ - Cl^- + Ca^{2+}} \quad (2.4)$$

CHAPTER 5
RESULTS AND DISCUSSION

The hydrogeochemical results from the existing database are presented in Table 5.2. The data were used to plot the Piper (Figure 5.3) and Durov diagrams (Figure 5.4). The water types deduced from the Piper plot, as well as the hydrogeochemical processes suggested from plotting the Durov diagram, are discussed. Table 5.3 shows stoichiometric ratios which were calculated using the major ion concentrations in milli-equivalents/l. The ratios were used to investigate the possible sources of the major ions in the groundwater samples. Figure 5.2 displays the correlation plots where major ions are plotted against one another to determine the processes that give rise to the ions in the groundwater Section 5.2.5 shows results and presents a discussion of geochemical modelling, whereas Table 5.4 reflects on the results of a saturation index. The last section of this chapter presents results and a discussion of environmental isotopes.

5.1 Reliability analysis

Table 5.1 displays the results of charge balance calculations obtained from 29 groundwater samples collected around the Frischgewaaged and Boschkoppie farms where RBplat is currently mining (Table 5.2). Of the 29 ion balance errors calculated for each borehole, three boreholes, BH08, BH12, and E12, yielded positive results which are less than 5%. This means that the cations are in excess and anions are insufficient (Duetsch and Siegel, 1997). Fourteen of the boreholes had ion balance error (IBE) values of less than 11.5% and 11 of the boreholes had values ranging from 12.4% to 50.8%. According to Schuster (2013), samples that have high ionic strength are prone to yielding an IBE of 10% and less and those with low ionic strength are prone to yielding IBE between 10% and 20% but are still valid. All borehole samples that yielded an IBE higher than 11.5% were classified as unreliable and therefore excluded from further analyses.

Table 5.1: Results of the ion balance error calculation

Borehole ID	Ion Balance Error %	Borehole ID	Ion Balance Error %
BH03	**12.4**	BRG11	**15.6**
BH04	**13.1**	BRG14	**19.2**
BH08	2.8	DWA05	9.0
BH09	6.2	E12	4.4
BH11	8.6	E15	9.8
BH12	3.0	E19	10.3
BH13	**19.3**	E21	**12.3**
BRG01	**51.0**	LF01	**28.5**
BRG03	9.5	LF02	9.8
BRG04	10.3	LF03	11.5
BRG05	**28.0**	R8	**12.9**
BRG08	**50.5**	R26	9.0
BRG09	10.1	R41	5.8
BRG10	11.9	UH45	9.6

Table 5.2: Hydrochemical parameters of groundwater within the Fidgewaagdt and Boschkoppie farms collected for groundwater-monitoring purposes (BRPM Environmental Database, 2018).

Borehole ID	Water level (m)	pH	EC mS/m	TDS mg/l	Ca mg/l	Mg mg/l	Na mg/l	K mg/l	Alkalinity as $CaCO_3$ mg/l	Cl mg/l	SO_4 mg/l
BH07	4.3	8.3	232.9	1842.6	25.0	344.6	52.4	2.3	289.0	181.7	976.5
BH08	7.2	8.1	116.5	694.4	32.7	111.0	67.7	0.4	424.7	78.0	142.2
BH09	13.8	7.8	61.3	357.6	43.4	8.4	87.6	1.3	314.6	7.9	12.1
BH11	8.3	8.0	185.2	1222.9	29.8	235.0	46.7	0.7	485.0	130.7	475.3
BH12	10.0	7.7	126.9	676.0	62.5	124.8	16.4	1.3	342.9	52.8	117.8
BRG03	10.7	7.5	61.4	336.9	34.0	54.6	14.1	2.1	298.2	12.3	16.5
BRG04	13.4	7.8	136.1	706.9	58.8	127.2	39.3	1.0	396.3	23.2	65.2
BRG09	20.9	8.2	82.9	466.9	53.1	33.9	77.7	2.9	304.8	28.5	57.8
BRG10	14.5	7.9	125.0	694.9	55.1	104.5	65.4	0.9	471.0	41.7	70.7
DWA05	1.9	8.3	167.9	1221.0	65.0	174.4	83.7	1.4	298.0	107.3	555.7
E12	0.0	7.9	46.5	252.2	244	42.7	9.8	1.0	203.9	13.5	25.5
E15	0.0	7.7	32.8	171.5	24.0	24.5	6.0	1.3	140.0	11.1	3.4
E19	0.0	7.9	46.7	318.2	23.6	42.6	8.8	0.9	202.4	11.8	23.2
LF02	21.8	8.1	89.8	505.9	65.5	64.9	33.6	2.3	393.1	33.8	44.3
LF03	19.2	7.9	71.5	397.0	31.5	75.9	16.6	0.6	351.8	10.8	34.6
R 26	0.0	11.1	70.1	394.4	37.2	61.2	27.6	4.6	314.9	32.1	37.3
R 41	1.7	8.2	70.0	370.4	39.2	25.4	57.0	8.1	115.6	89.0	76.6
UH45	11.1	7.7	90.0	493.7	55.7	58.4	55.6	1.6	473.4	11.0	10.7

5.2 Groundwater-monitoring boreholes – Royal Bafokeng Platinum Mine

Prior to using data from monitoring boreholes (Table 5.2), the data were averaged out to avoid the seasonal effects on water chemistry. According to Masindi and Abiye (2018), this averaging makes the identification of hydrogeochemical processes and the evolution of groundwater possible.

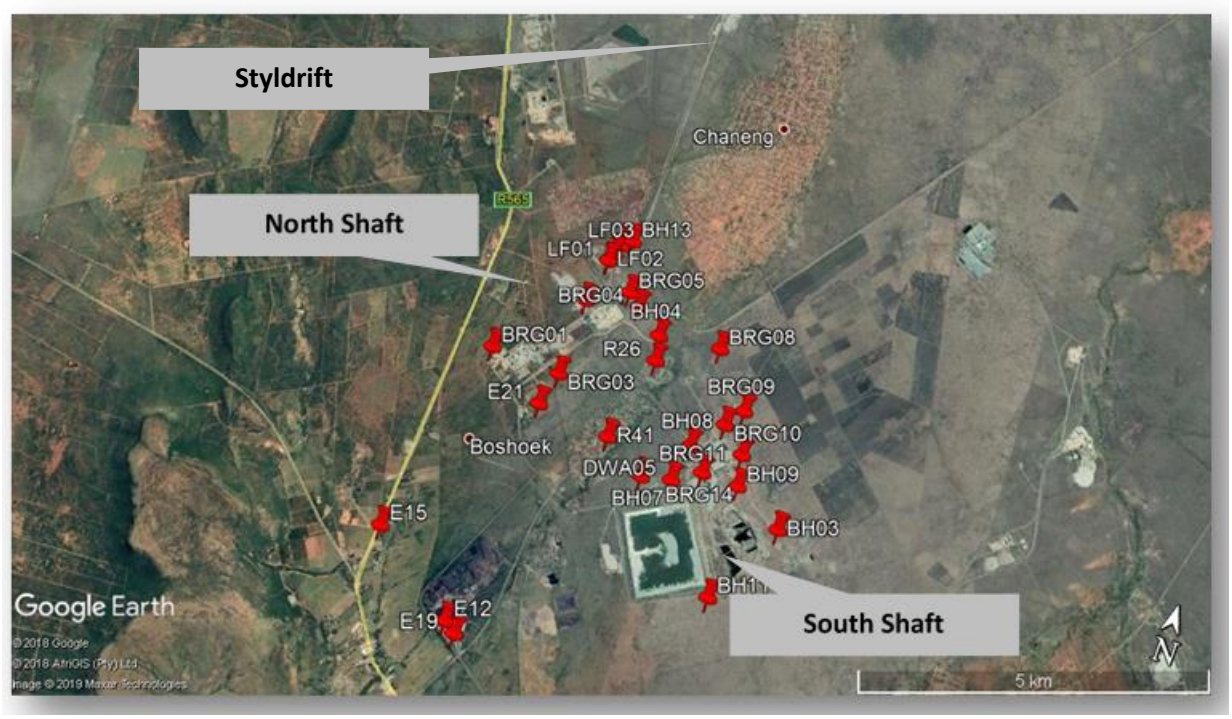

Figure 5.1: Google Earth image showing the locations of the monitoring boreholes in the RBplat area.

5.2.1 Physiochemical and chemical properties

Table 5.2 shows the physicochemical and chemical properties of water collected from the water-monitoring stations around the RBplat mining area (Figure 5.1). The pH ranged from 7.4 to 11.1. BH13 had the highest EC value, which is 334.8 mS/m, and the second-highest TDS value at 1740 mg/l. The reason for this is the proximity of the borehole to a landfill site. The lowest record of EC was 32.8 mS/m measured at borehole E15. The TDS value of 1842 mg/l at BH07 was the highest recorded of the 29 samples, while sample E15 had the lowest TDS at 171 mg/l. These boreholes are situated 3.7 km and 4 km from underground operations, respectively.

The concentration of major cations and anions is presented in Figure 5.2. From each ion, the concentration is presented in descending order. General observation shows groundwater

samples with the highest ion concentrations at the discharge zones while the groundwater samples at the recharge zones have the lowest ion concentration. The concentration of these ions shows an increasing trend of Na, Mg and Ca downstream. The sulphate and chloride concentrations do not follow a trend with the flow path, instead, they increase in concentration closer to the tailings. This is an indicator that water has been affected by anthropogenic sources (mining sources).

The ion chemistry for cations in the groundwater is as follows Mg>Ca>Na>K, and anions HCO_3>SO_4>Cl. This reflects the mineralogy of the area as discussed in section 3.1, Mg silicates are the most abundant while potassium-bearing silicates are the least abundant and occur as trace minerals.

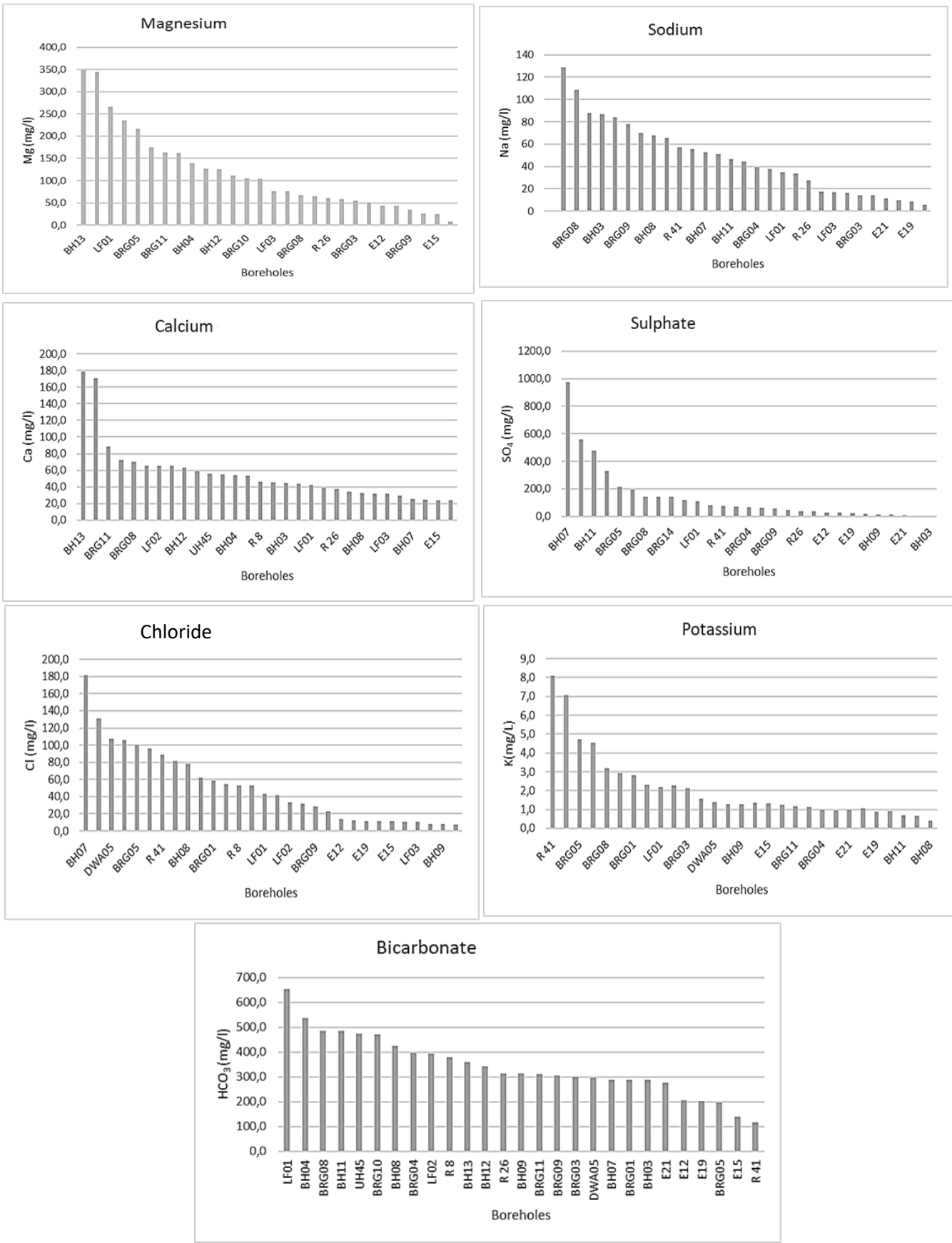

Figure 5.2: Concentration of major ions (mg/l).

5.2.2 Water type classification

Based on the Piper plot in , three water types, namely; magnesium bicarbonate, magnesium sulphate and mixed water type were identified. The magnesium bicarbonate water type was found to be the most dominant form all the samples, followed by the magnesium sulphate water type.

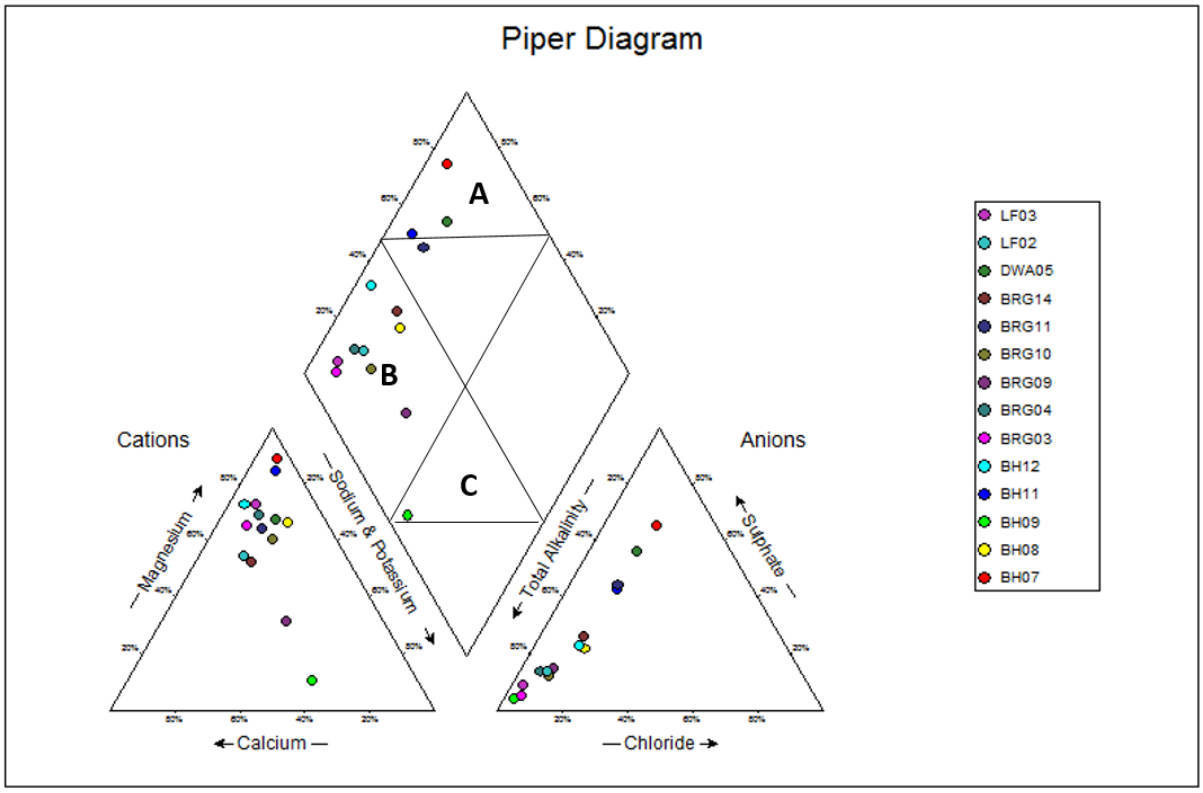

Figure 5.3: Piper diagram showing the average composition of major ions of groundwater samples collected around RBplat-created by WISH

Figure 5.4 : RBplat map showing the rivers running through the area as well as the exact locations of the boreholes used for sampling. 2019 samples collected at North Shaft where the are is demarcated by a red circle.

***Magnesium bicarbonate water type* (B)**

Over 50% of the groundwater samples are Mg-HCO_3 water type. As highlighted in section 3.1 and 3.2, fractures are a major part of the groundwater system in RBplat. Fractures play an important role in the groundwater system around RBplat because the crystalline rocks are made porous by fracturing due to their brittle nature. Groundwater circulates and stored in fractures that are often partially infilled by secondary silicates with high Mg content. The water table in this area lies in the weathered zone of pyroxenite and talc, this means consistent water-rock interaction with ferromagnesian minerals. The water type is attributed to the interaction of infiltrating water with magnesium bearing minerals.

***Magnesium sulphate water type* (A)**

BH11, BH07 and DWA05 reflect the magnesium sulphate water type. These groundwater samples were collected from boreholes that are located near tailings dams and abandoned open pits. A common indication of groundwater pollution by industrial waste is an elevated concentration of chloride and sulphate (Swaminathan and Venkatesan, 2000). This was noticed in the groundwater near tailings dams around RBplat as affected by leachate and displays an increased content of sulphate and chloride. Unlike other ions, the increase in the concentration of sulphate ions does not follow a flow path but rather proximity to the tailings.

During ore separation and treatment processes, reagents such as hydrochloric acid and sulphuric acid are used for the effective extraction of PGEs. Following the treatment process, the wastewater from the RBplat concentration plant is discharged into the tailings dam. The PGEs in the area commonly occur with base metal sulphides such as pyrrhotite and chalcopyrite which are later disposed of as gangue material at the tailings. The sulphide and chlorine-bearing leachate from these tailings into the groundwater give rise to Mg-Cl-SO_4 water type.

***Mixed water type* (C)**

The mixed water type was obtained from two boreholes, BH09 (Na-Ca-HCO_3) and BRG11 (Mg-HCO_3-SO_4). The chemistry of the two boreholes show traits of stagnant water or an isolated aquifer. The TDS in BH09 sample is 357.6 mg/l which is below an average of 736.3 mg/l for all the samples. All the other ions are also below average except for Na which is high at 87.6 mg/l. Elevated concentration of Na could be attributed to recharge from a long time ago

which was affected by evaporation. For BRG11, fresh meteoric groundwater got mixed with sulphate-bearing leachate from the tailings dam.

Figure 5.4 shows groundwater samples around RBplat on a Durov plot. The majority of the samples have high concentrations of HCO_3^-, Ca^{2+} and Mg^{2+}. The water type with these three ions dominating indicates interaction with mafic igneous rocks which are abundant in the RBplat area (presented in section 3.1). BH07, BH11, DWA05 and BRG11 plot on the field where neither cations nor anions are dominant. These are groundwater samples collected near tailings dams and have high sulphate (555.7 mg/l -976.5 mg/l) and magnesium contents (163.5 mg/l-348.7 mg/l). This water type is associated with mixing and/or sample dissolution.

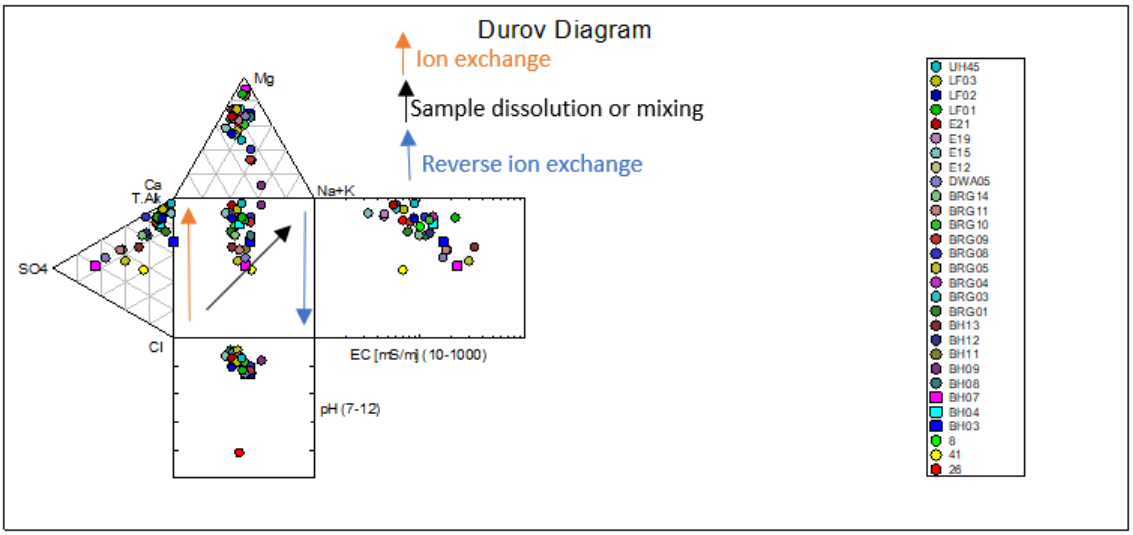

Figure 5.4: Durov plot of the groundwater samples around RBplat.

5.2.3 Water rock interaction

The stoichiometric ratios in table 5.3 which were calculated using equation 2.1 disqualify the dissolution of halite as a possible process in the groundwater, however, 50% of the samples have r<1 and the remaining 50% has r>1. This indicates that silicate weathering has played a substantial role in controlling the ion chemistry of the water.

The results presented in table 5.3 based on equation 2.2 show the majority of the ratios are >0.5, while only four (BH07, BH08, BH11 and DW0A5) samples have r<0.5. As explained in section 2.4, ratios >0.5 indicate that the calcium ion in the water is as a result of carbonate or silicate weathering rather than gypsum. For the four samples with r>0.5 it indicates that

calcite precipitation took place where calcium was removed. The results from equation 2.3 have r<1 for all the water samples. This indicates that the groundwater is from fresh recharge of meteoric origin.

Table 5.3: Stoichiometric ratios (Ratio calculated in meq/l).

	$\frac{Na^+}{Cl^-}$	$\frac{Ca^{2+}}{Ca^{2+}+SO_4^{2-}}$	$\frac{Ca^{2+}+Mg^{2+}}{HCO_3^{2-}}$	$\frac{Mg^{2+}}{SO_4^{2-}}$	$\frac{Na^+ + K^+ - Cl^-}{Na^+ + K - Cl^- + Ca^{2+}}$
BH07	20.34	0.06	0.04	1.39	1.81
BH08	2.96	0.35	0.10	3.08	0.32
BH09	0.25	0.90	0.37	2.72	0.63
BH11	9.9	0.13	0.05	1.95	10.98
BH12	2.45	0.56	0.20	4.19	-0.31
BRG03	0.34	0.83	0.18	13.1	0.16
BRG04	1.36	0.68	0.17	7.7	0.27
BRG09	1.2	0.69	0.34	2.32	0.50
BRG10	1.47	0.65	0.17	5.84	0.38
DWA05	11.58	0.22	0.17	1.24	0.17
E12	0.53	0.70	0.18	6.6	0.06
E15	0.07	0.94	0.28	28.15	-0.02
E19	0.48	0.71	0.17	7.24	0.06
LF02	0.92	0.78	0.28	5.79	0.15
LF03	0.72	0.69	0.13	8.67	0.22
R26	0.78	0.70	0.18	6.47	0.18
R41	1.6	0.55	0.49	1.31	0.08
UH45	0.22	0.93	0.22	21.59	0.44

5.2.4 Bivariate analysis

The correlation coefficients were classified based on the Guildford rule of thumb (Gildford, 1973) which is explained in section 4.7. All the results have negligible correlation except for magnesium vs sulphate which has a moderate correlation.

Table 5.4: Correlation coefficients for bivariate plots.

Bivariate plot	Correlation value	Classification
Ca^{2+} vs SO_4^{2-}	0.004	Negligible
Ca^{2+} + Mg^{2+} vs HCO_3^-	0.07	Negligible
Na^+ vs Cl^-	0.12	Negligible
Mg^{2+} vs SO_4^-	0.5	Moderate

5.2.4.1 Ca/SO_4

The Ca^{2+} vs SO_4^{2-} plot was constructed to determine the sources of calcium and sulphate ions in the water. According to Jalali (2007), samples that plot along the 1:1 line indicate the dissolution of gypsum as the source of both calcium and sulphate. For the samples plotted in Figure 5.5, there is no correlation between the two ions and no samples were plotted along the 1:1 line. This disqualifies the dissolution of gypsum as the source of the two ions and this is in line with the geology of the area because there is no occurrence of gypsum. The correlation plot, however, shows that there is more calcium over sulphate in the majority of the groundwater samples. An explanation for this could be that calcium is coming from the weathering of carbonate minerals rather than silicate minerals (Hounslow, 1995). The process responsible for the calcium ions in the samples is the weathering of fluorite. According to Ahmed and Saxena (2001), the dissolution of fluorite takes place in alkaline waters with pH of 7.6 to 8.6 and high HCO_3 concertation and this is the case with the groundwater around the mine. The few samples that plotted above the 1:1 line are more enriched in sulphate and according to Kozlowski and Komisarek (2016).

The molar ratio of Ca/SO_4 was calculated and presented in Table 5.3. This was also done to determine the sources of calcium and sulphate in the groundwater samples. The molar ratio of $r= 0.5$ indicates dissolution of gypsum and $r> 0.5$ indicates other sources of calcium such as carbonates or silicates weathering, while $r<0.5$ and a neutral pH may indicate the removal of calcite through calcite precipitation (Hounslow, 1995). The molar ratio results are in line with the correlation plot as the majority of the ratios are more than 0.5 which indicates the addition of calcium through the weathering of fluorite. The few samples with $r<0.5$ are a result of calcite precipitation which reduces the calcium in the water.

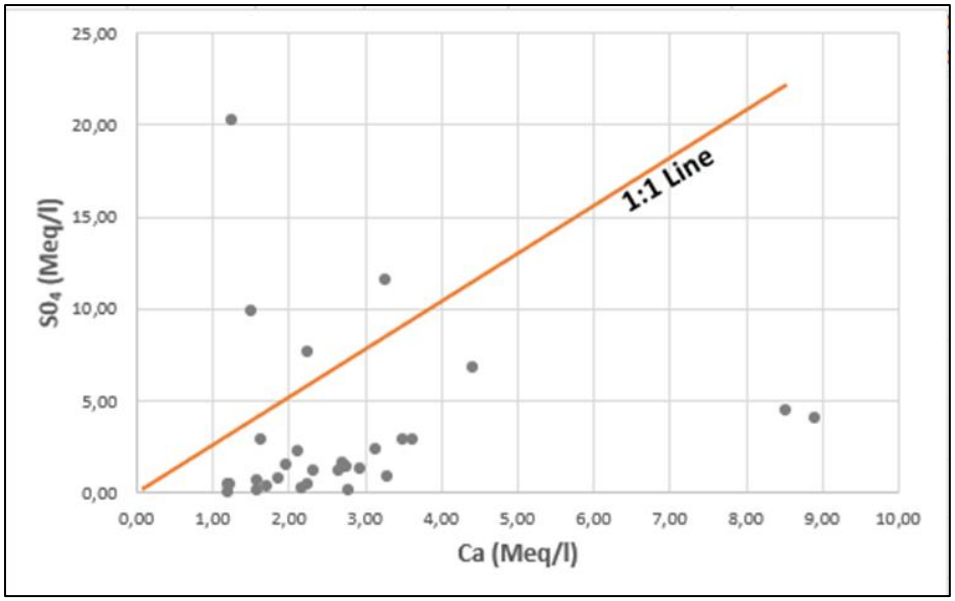

Figure 5.5: Ca vs SO_4 bivariate plot for the groundwater samples.

5.2.4.2 Ca+Mg/ HCO_3

A correlation plot of Ca+Mg and HCO_3 was constructed because over 50% of the groundwater samples in the area are of Mg-HCO_3 water type. Furthermore, stoichiometric ratios for Ca+Mg/HCO_3 were calculated and presented in Table 5.3. This was done to determine the hydrogeochemical processes and sources responsible for the ion chemistry in the water samples. For all the samples presented in Figure 5.6 and Table 5.3, the Ca+Mg/HCO_3 ratio is <1 which indicates that the ions in the groundwater can be attributed to silicate weathering and the groundwater was recently recharged by rainfall. According to Akpofure and Okiongbo, (2014), the samples that are plotted above the 1:1 equiline on the Ca+Mg and HCO_3 diagram are a good indication that the presence of Alkali Earth materiasl in the water is as a result of silicate weathering over bicarbonate, however, the groundwater samples in Figure 5.6 plot below the 1:1 line indicating a predominance of HCO_3 as opposed to silicate weathering.

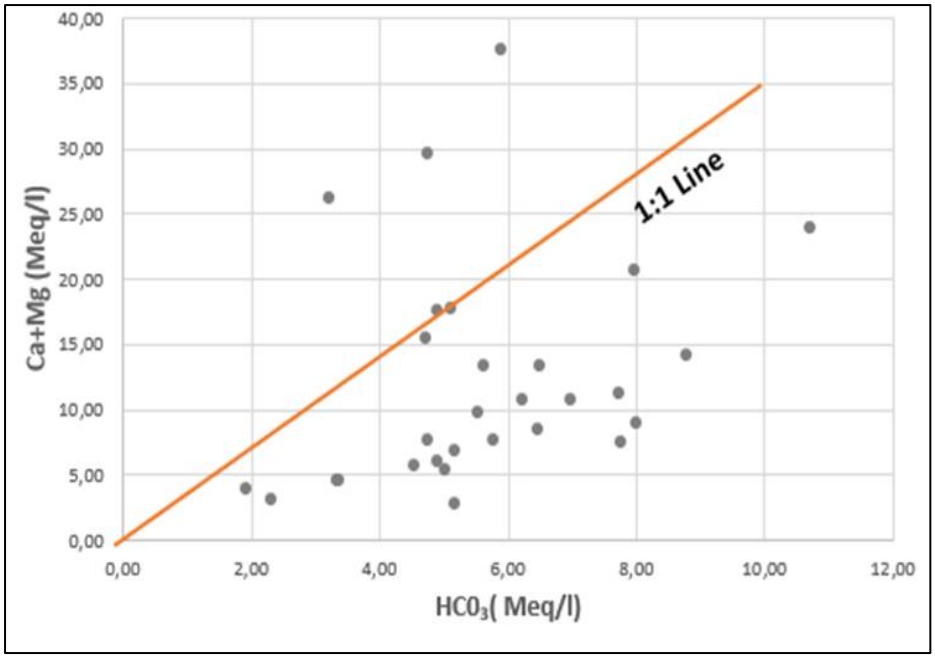

Figure 5.6: Ca+Mg vs HCO_3 bivariate plot for groundwater samples.

5.2.4.3 Na/Cl

The Na vs Cl correlation plot is presented in Figure 5.6 and the molar ratios of Na/Cl are presented in Table 5.3. Samples that plot directly on the 1:1 equiline indicate halite dissolution and samples that plot below or above the 1:1 equiline indicate other processes rather than halite dissolution (Lakshmanan et al., 2003; Zaidi et al., 2015). The Na/Cl molar ratio which is equal to 1 suggests the dissolution of halite, greater than 1 suggests silicate weathering while less than 1 is an indicator of processes such as ion exchange (Jalali, 2009).

The majority of the samples in Figure 5.7 plot below the 1:1 line and they have a molar ratio >1. For these samples, sodium is enriched as a result of silicate weathering of sodium-rich feldspar. While silicate weathering is the primary process responsible for the sodium content in the water samples, the outliers indicate the possible occurrence of other processes contributing to the sodium and chloride ions in the water. The groundwater samples that are plotting above the 1:1 line show more chloride ions over sodium ions which indicates the removal of sodium through ion exchange (Elango et al., 2003; Jalali 2007).

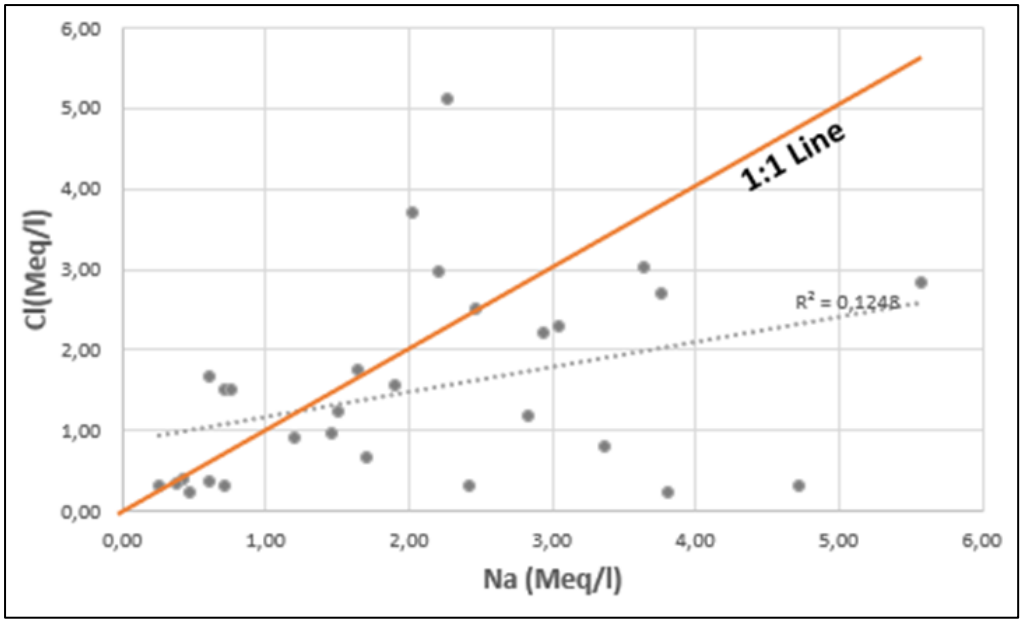

Figure 5.7: Na vs Cl correlation plot for analysed groundwater samples.

5.2.4.4 Mg/SO_4

The magnesium sulphate water type is the second most dominant water type among the samples, and it is observed on polluted boreholes which are close to tailing facilities. Magnesium against sulphate was plotted (Figure 5.8) to identify the processes that contributed to the water type. The occurrence of this water type is as a result of the mixing of freshwater with sulphate rich leachate from the tailings and landfills. Most samples plot below the 1:1 line and this means there is magnesium in the groundwater. Having more magnesium suggests more than one source contributing to the magnesium ions in the water.

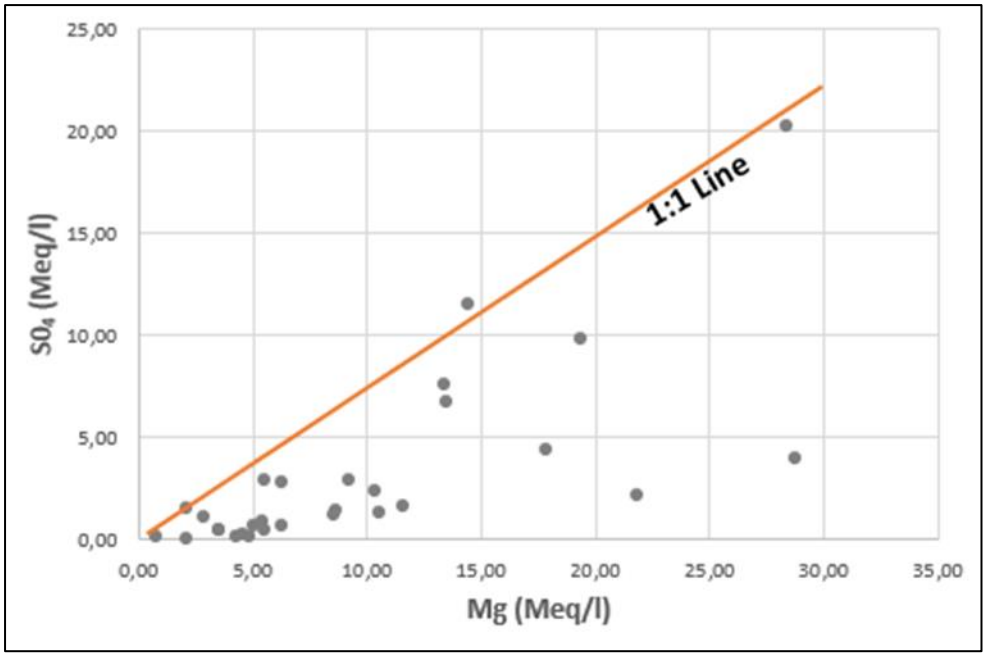

Figure 5.8: Mg vs SO_4 correlation plot for analysed groundwater sample.

5.2.3.6 Carbonate weathering

Based on the results of bivariate plots as well as the Durov plot, carbonate precipitation has been confirmed as one of the processes taking place in the system (Equation 5.1). On the other hand, the saturation index results show calcite precipitation among other carbonate minerals as one of the processes taking place in the system. Calcite is very ubiquitous around RBplat area and it is commonly found as an infilling in geological fractures and joints. Equation 1 shows the precipitation of calcite.

Ca^{2+} (aq) + CO_3^{2-} (aq) $\leftrightarrow CaCO_3\ (s)$ (5.1)

5.2.3.7 Silicate weathering

Unlike carbonate weathering, silicate weathering takes place at a slow pace because of the nature and hardness of silicate minerals (Equation 5.2 and 5.3) (Appelo and Postma, 2005). Some of the bivariate plots and stoichiometric ratios revealed silicate weathering to have contributed to the presence of some of the ions in the water. According to Hounslow (1995), if molar ratios calculated for silicates in Table 5.3 are <0.2 and >0.8 it is less likely for silicate weathering to take place and when the ratio is between 0.2 and 0.8, silicate weathering can be considered in contributing to the groundwater chemistry change.

BH08, BH09, BH11, BRG03, BRG04, BRG09. BRG10, DWA05, E12, E19, LF02, LF03, R26, R41, UH45 have molar ratios which are >0.2 and <0.8 which confirms the occurrence of silicate weathering as a primary process that contributed Na^+, K^+, Cl^- or Ca^{2+} to the system. Equation 5. 2 shows the weathering of anorthite in the presence of carbonic acid in water; the end products are kaolinite, calcium and bicarbonate ions (Clark, 2015).

$$CaAl_2Si_2O_8\ (s) + 2H_2CO_3\ (l) + H_2O\ (l) \rightarrow Al_2Si_2O_5(OH)_4\ (s) + Ca^{2+}\ (aq) + 2HCO_3^-\ (aq) \qquad (5.2)$$

$$3NaAlSi_3O_8\ (s) + H_2O\ (l) + Mg^{2+}\ (aq) \rightarrow 2Na_{0.5}(Al_{1.5}Mg_{0.5})Si_4O_{10}(OH)_4\ (s) + 2Na^+\ (aq) + H_4SiO_4 \qquad (5.3)$$

5.2.5 Saturation indices

shows the plan view of the study area and its elevation profile. The surface elevations and groundwater levels from the borehole samples were used to determine the flow direction of the groundwater in the area. The groundwater flow is generally from the south towards the north of RBplats (the hydraulic head decreases towards the north) The groundwater was not analysed for SiO_2, and the study area is highly mineralized by silicates. The saturation index results will therefore have an overemphasis on some metal oxides because in addition to the major ions, Fe and Mn were analysed.

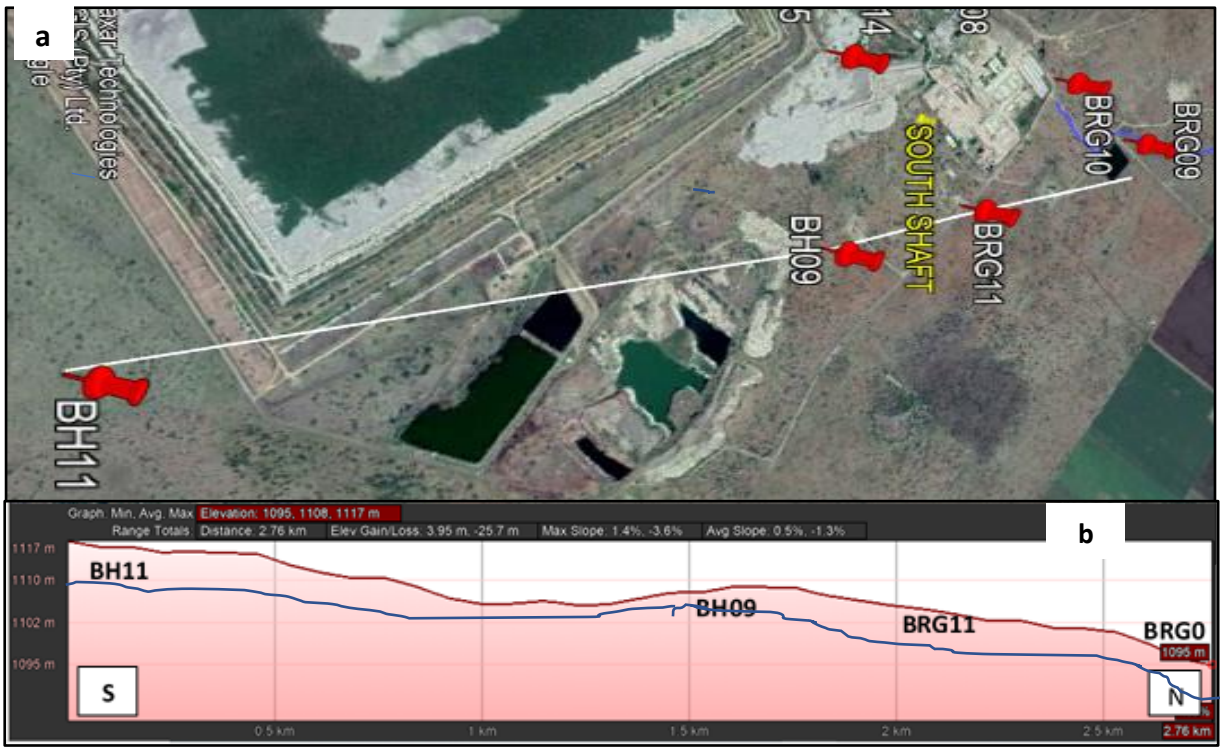

Figure 5.9: (a) Plan view of the selected flow path. (b) Section view of the selected profile showing the ground surface and the water table.

Table 5.5: Saturation indices calculated using phreeqc.

Minerals	Formula	BH11	BRG03	BRG04	BRG09	BRG10	BH09
Aragonite	$CaCO_3$	0.39	-0.05	2.90	0.80	0.66	0.4
Anhydrite	$CaSO_4$	-1.99	-3.04	-0.06	-2.33	-2.37	-3
Gypsum	$CaSO_4{:}H_2O$	-1.69	-2.69	0.23	-2.03	-2.07	-2.69
Dolomite	$CaMg\ (CO_3)_2$	2.30	0.75	6.58	2.05	2.23	0.72
Calcite	$CaSO_3$	0.53	0.10	3.05	0.95	0.8	0.54
Fluorite	CaF_2	-	-	-0.55	-3.22	-	-
Halite	NaCl	-6.84	-8.33	-4.99	-7.24	-7.16	-7.72
Rhodochrosite	MnO_2	0.20	0.16	-	-	0.47	0.09

Note (-) = No content from phreeqc results.

The SI results show an under-saturation of gypsum which suggests that the gypsum precipitation cannot happen in the groundwater. This hypothesis is also supported by the molar ratio calculations as well as the correlation plot which displayed no correlation between the two ions and the molar ratio is over 0.5 which is as a result of fluorite dissolution.

According to the results, the groundwater is under-saturated with respect to halite and therefore, Na and Cl still exist in solution. The correlation plot of sodium versus chloride as well as the molar ratio results supports this hypothesis. The plot and molar ratio calculation suggest feldspar weathering as the process which contributed to the ions in the water.

The SI results show oversaturation of dolomite, however, there is no geological evidence of the occurrence of dolomite in the study area. The positive SI results suggest that if favourable conditions are provided, dolomite will be precipitated. The conditions in the area are not favourable to the precipitation of dolomite therefore the results are rejected.

Calcite and aragonite saturation index results show oversaturation of both minerals but due to its stable conditions, calcite is the polymorph that occurs in the area. The oversaturation of calcite presented on the SI results is in line with the geological evidence in the area. Calcite is ubiquitous in RBplat and it is dominantly found infilled in joints and fractures as seen in Figure 3.4 in chapter 3.

5.3 Hydrogeochemical processes around storage tailing facilities

As previously highlighted, the most dominant anion in this groundwater system is the bicarbonate ion. This is not uncommon because, in most of the natural surface and groundwater systems, sources of bicarbonate ions are ubiquitous. Interaction between the atmosphere, surface and groundwater make the whole system a carbonate system. Groundwater with high bicarbonate content is an indication of water near the outcrop; the deeper and further the groundwater is from the outcrop, the less bicarbonate it contains (Hiscock, 2005).

5.3.1 High sulphate content

Figure 5.10: Samples near landfills and tailings showing elevated sulphate content (Google Earth, 2020).

Sulphate is the second most abundant anion in natural waters, led by HCO_3^- (Hem, 1985). In several environmental systems, the geochemistry of sulphur has primary control over redox reactions. Even though the source of sulphate in water is natural, in many cases the elevated sulphate content is due to anthropogenic sources. Natural sources of sulphate include atmospheric deposition and dissolution of sulphide minerals. Human influenced sources of sulphate include waste dumps, landfills, power plants and smelters (Brusseau et al., 2011).

As shown in Figure 5.10, boreholes BH07, DWA05, BH11 and BRG05 are all located less than a metre from the tailings in different directions. The groundwater samples from these boreholes do not only have the highest sulphate content but also have the highest TDS, EC and chloride

content. The water level in these boreholes is very shallow ranging between 1.9 m.b.s and 10.4 m.b.s which suggests additional flow around the area.

From the correlation, Piper and Durov plots, these water samples indicate mixing to have resulted in their water chemistry. Mixing occurs between fresh meteoric groundwater which is Mg-HCO_3 and later changes to Mg-Cl-SO_4 as it interacts with the sulphide bearing leachate from the tailings. Apart from mixing, the oxidation process can be assumed to be taking place around the tailing as the sulphide bearing gangue which was initially not exposed to oxygen is now exposed to oxygen on the ground surface.

The PGMs are hosted by sulphide bearing platinum ore and during the ore separation process, the PMGs of interest are recovered and sulphide bearing ore becomes part of the gangue which is sent to tailings facilities as part of the slurry (Goncharov et al., 2004). As part of the recovery of PGMs, HCl and H_2SO_4 are added as part of the flotation process (Goncharov et al., 2004). Once the process is complete, the slurry which contains the HCl and H_2SO_4 as well as the sulphide bearing gangue is discarded into landfills and storage facilities around the mining area.

5.4 Underground sampling data – North Shaft

This part of the project was carried out to determine the source of water that was intersected in some parts of the underground workings during the mining process. Water ingress negatively affects the underground workings as it hinders production when it floods the areas. In other cases, the water pressure is so high and constant that it exerts excessive pressure on the fractures through which the water circulates. A flooded mining area poses danger, including drowning and high water pressure. Excessive water pressure in geological fractures exacerbates poor ground conditions.

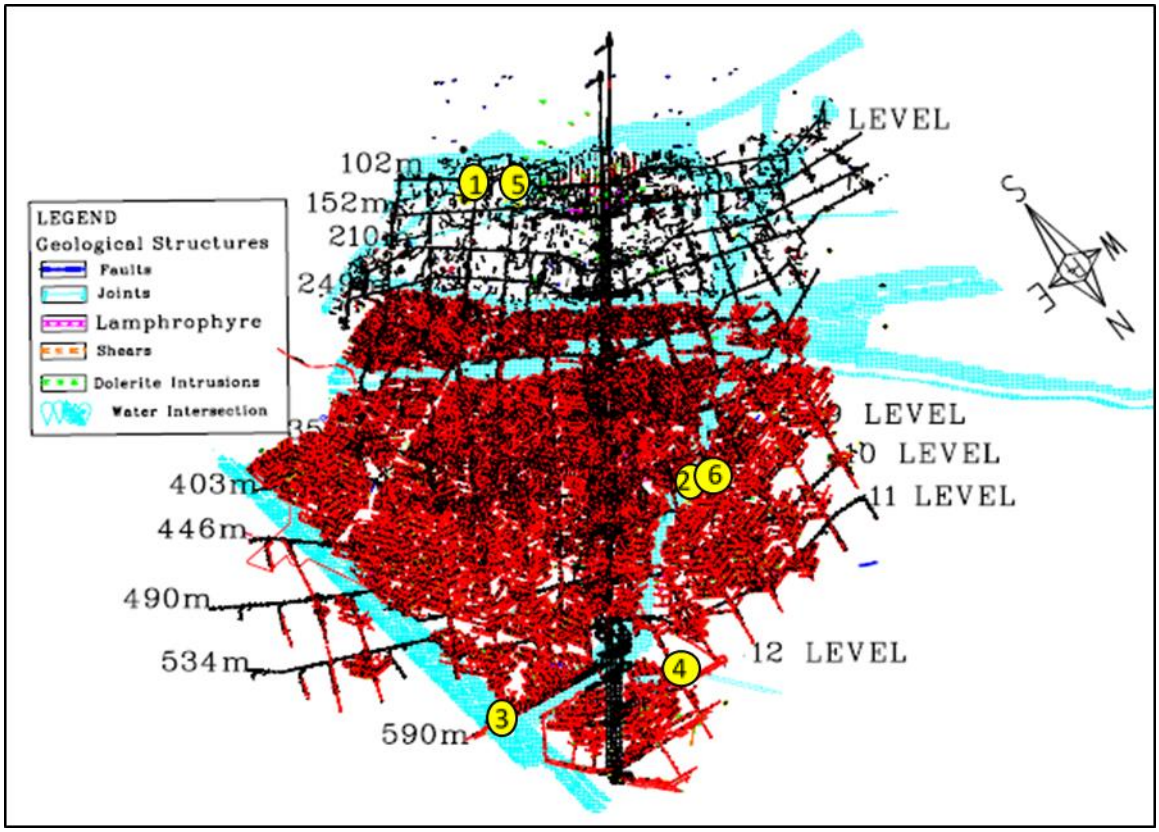

Figure 5.11: Plan view of North Shaft including underground sampling points and water bearing zones (Source: RBplat Micro-station). The numbers in yellow circles indicating different sampling points in the mine (Underground).

Figure 5.11 shows a plan view of the North Shaft of RBplat where six water samples were collected for chemical and stable isotope analysis to investigate the primary source of the intersected water. The shaft is currently mining from 1 level to 16 level (depth increases with levels). The water samples were collected between 1 level (102 m.b.s) and 13 level (590 m.b.s) at different intersection points. The red polygons show mined-out reef areas, while the blue ones show water-bearing zones. The blue shades in the map are water-bearing zones and areas where water was intersected underground. The black shades are mined-out areas which are off reef developments. Figure 5.12 shows the same mine plan with sampling points and geological structures.

5.4.1 Groundwater and geological structures

When major geological structures are intersected by mining, there is often water dripping or flowing out of the fractures. In other intersections, water flow eventually stops or decreases significantly, but in a few cases, the flow is consistent.

Figure 5.13 shows the plan view of the North Shaft and six sampling points, as well as the geological structures intersected. Dolerite intrusions are symbolised by green and shears are symbolised by orange. Blue lines denote the faults and blue polygons are patches of complete iron-rich ultra-mafic pegmatoids (IRUP). Partial IRUP patches are indicated by turquoise polygons. The structures that appear to be smaller in size are localised intersections with fewer effects of fracturing, while big structures are regional geological structures that tend to cause major disturbances in the area (for example; a regional fault will have a highly fractured ground, high displacement effect on the stratigraphy and high water outflow). The geological structures generally trend in different directions, but the common intersections are northwest-southeast and northeast-southwest, with dip angles ranging between 5° to 90° in different directions.

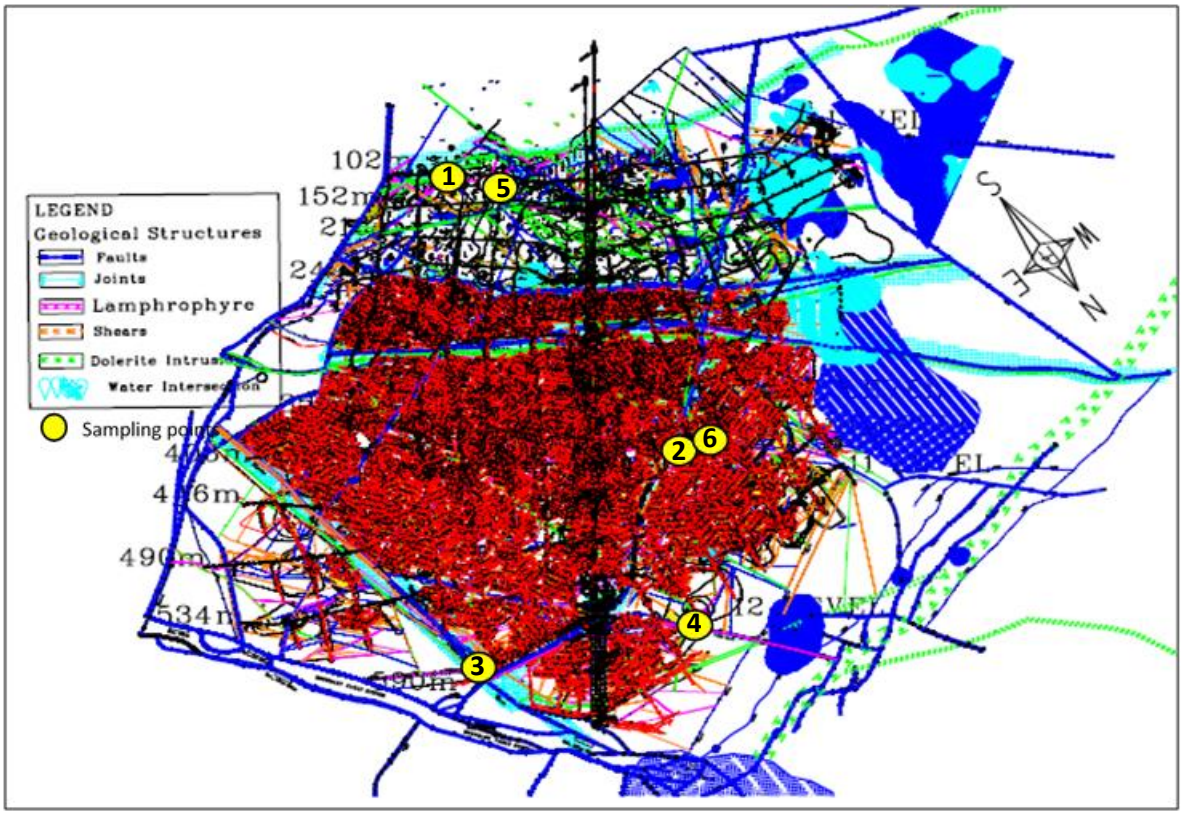

Figure 5.12: Plan view of North Shaft showing sampling points and geological structures (RBplat Micro-station).

To manage water ingress in the mine voids, some mining crews pump the water out and in other cases redirect or plug the water. Solutions for water ingress management are helpful when the original water source is known, hence investigation of the origins was central to the current work. Three samples were collected directly from the place where leaking took place (Figure 5.13 and Figure 5.14). The other two samples were collected from pipes that were used to

redirect the water. The last sample was taken from an underground drinking water tap (used as a reference). To determine the source of these waters, stable isotope analyses were carried out for the six samples.

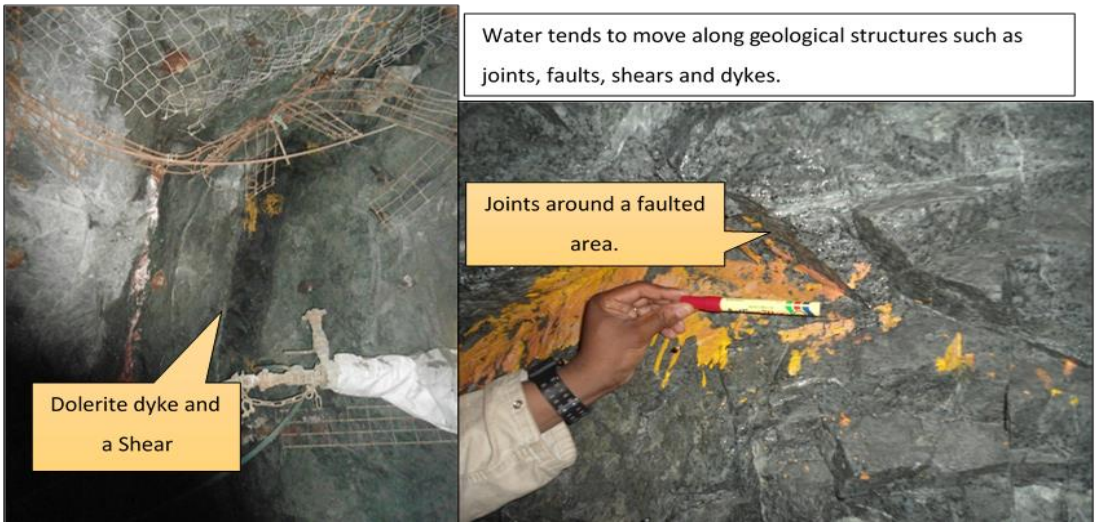

Figure 5.13: Water seepage along geological structures.

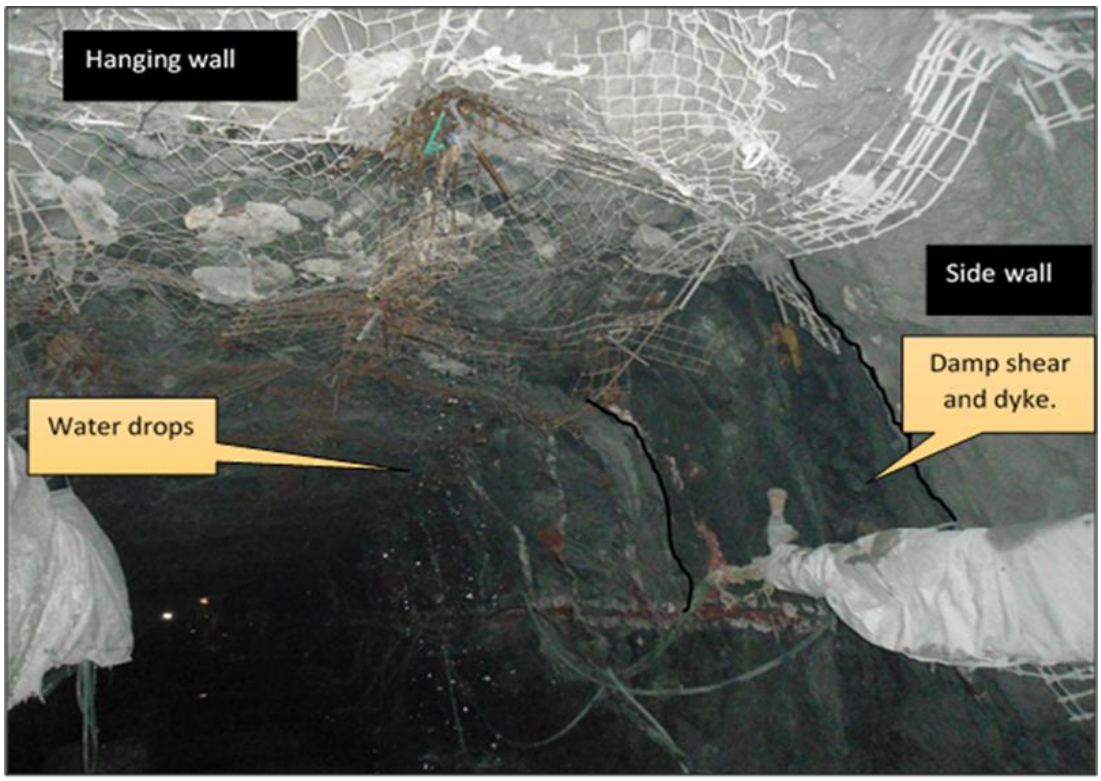

Figure 5.14: Water dripping from a regional dolerite dyke and shear.

5.4.2 Water chemistry of underground samples

Table 5.6 shows the water chemistry of the six water samples collected from the underground at the North shaft. The sample ion concentration is in mg/l and it was converted to meq/l to construct the piper plot in figure 5.15. The main picture in figure 5.15 is of the six samples and the insert is of the used groundwater data from the existing mine database.

Table 5.6: Water chemistry of six samples collected underground at North Shaft.

Sample ID	pH	EC (mS/cm)	TDS (mg/l)	Ca (mg/l)	Mg (mg/l)	Na (mg/l)	K (mg/l)	ALK (mg/l)	Cl (mg/l)	SO_4 (mg/l)	F (mg/l)	Al (mg/l)	Mn (mg/l)
Sample 1	7.12	97.60	983.71	112.00	23.00	113.00	2.74	480.00	46.00	58.00	0.70	0.27	148
Sample 2	7.50	78.70	669.93	76.00	74.00	27.00	2.93	320.00	89.00	79.00	0.16	0.50	0.74
Sample 3	9.80	125.70	882.19	23.00	0.08	258.00	2.59	9.00	272.00	316.00	0.10	0.15	1.27
Sample 4	9.66	104.30	627.57	15.70	0.44	204.00	5.26	9.00	91.00	294.00	0.20	0.58	7.39
Sample 5	7.00	111.00	878.27	60.00	129.00	36.00	2.82	500.00	78.00	71.00	0.50	0.15	0.80
Sample 6	6.52	1.82	585.85	32.00	24.00	61.00	11.60	190.00	170.00	76.00	0.10	0.15	21

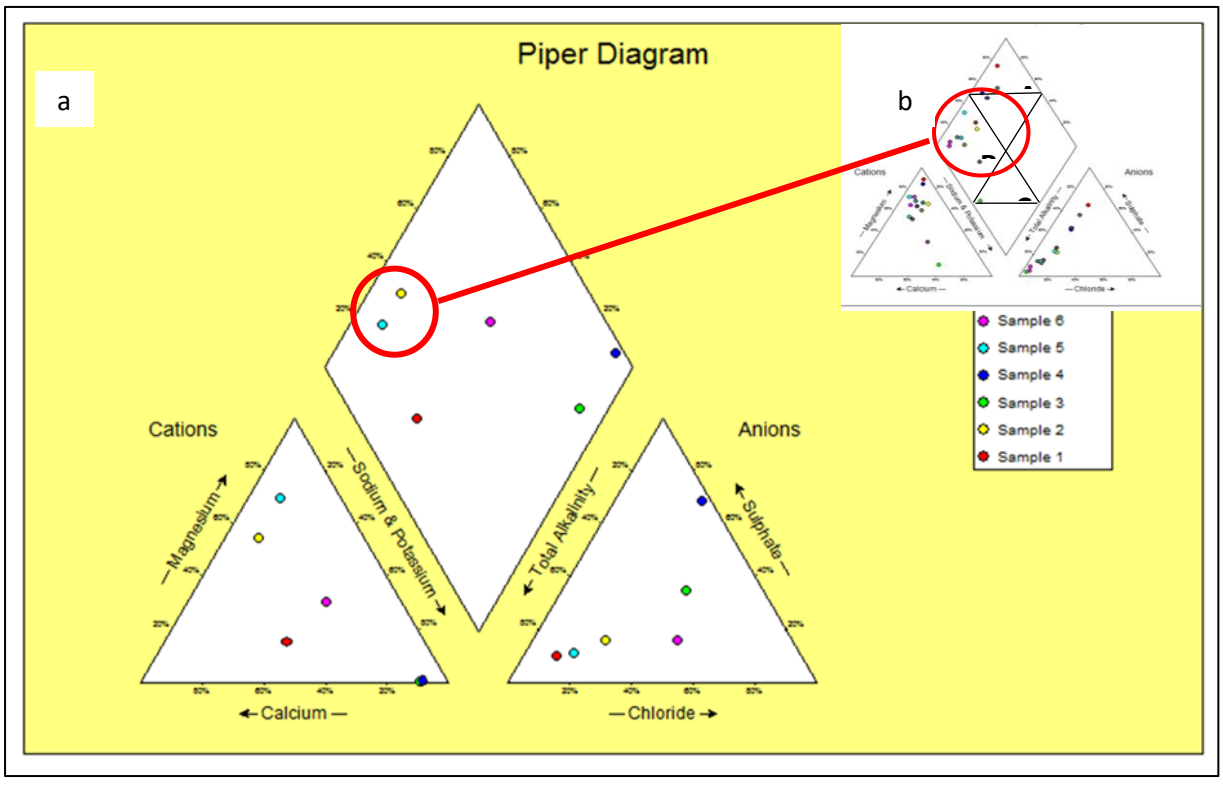

Figure 5.15: (a) A piper plot of 6 water samples collected from underground workings. (b) Insert: Piper diagram showing the average composition of major ions of groundwater samples collected around RBplat- created by WISH (see Figure 5.3).

Sample 1 - Na-Ca-HCO_3

The water sample was collected from a fault that cuts through pyroxenite. The rock is supported by rusted wire mash and roof bolts. At the time of the sampling, the flow rate of water was 5.4 ml/s. The water was clear in appearance with no odour. This sampling point is the nearest mining area to the ground surface, and it is 102 m below the ground surface where the UG2 reef is being mined.

Since the water was collected at 102 m below surface, which is over 50 m below the aquifer, it percolated further away from the oxic shallow aquifer into the deeper part of the ground where there is minimal oxygen hence the low ORP (-30 mV) was recorded.

Sample 2-Ca -Mg-HCO_3

The sample was collected from a large water pipe. The pipe was installed to drain the water from the stopping areas above the excavation. The water was clear in appearance and had no odour. The flow rate of the water was fast since it filled a 250 mm bottle in less than 30 seconds. This sample plots in the same position as the majority of the groundwater samples on the Piper plot (Figure 5.15).

The biggest contributor to the hardness of water is Mg which was found to be 74 mg/l. In the BIC where major minerals that exist are ferromagnesium silicates, high content of magnesium is not unusual. Interaction of water and ferromagnesium minerals can result in high Mg and Ca in the water. Water rock interaction was confirmed by the Gibbs plot in Figure 5.16.

Sample 3 - Na-Cl-SO_4

The water sample was collected from the hanging wall excavation fractured by a regional shear, fault, lamprophyre, and dolerite dyke. The sampling point was at 518 m above sea level (Figure 5.11) which is 590 m below the ground surface. The collected water sample was dripping at a rate of 2.36 ml/s and it was light brown. The water had strong hydrogen sulphide like odour.

This water sample was dominated by sulphate> chlorine> sodium ions. From all the 6 samples that were collected as well as the groundwater monitoring samples, sample 3 and sample 4 have the lowest magnesium content and elevated sodium content.

With high levels of sulphate and a distinct odour, it is assumed that this water had undergone sulphate reduction. This is supported by Brusseau et al. (2011), where it is stated that the odour of rotten eggs in water is a typical indicator of the production of H_2S from the reduction of sulphate.

Sample 4- Na-Cl-SO_4

The water was collected from 13 level diagonal which is an excavation that is developed 610 m below the surface. The collected water was dripping from the hanging wall and sidewall where the excavation is cut by a fault and a lamprophyre dyke. The rate of flow of the water was low at 0.87 mm/s. The water was clear in appearance and had no odour.

The ion chemistry of this sample is similar to that of sample 3 calcium and magnesium are low with concentrations of 15.70 mg/l and 0.44 mg/l respectively. The sulphate and TDS contents are high at 294 mg/l and 878.27mg/l, respectively. The only difference in this sample is the high manganese content. Manganese is very popular in steel manufacturing; the possible source of manganese could be the drill rig or bolts which are used to support the hanging wall and sidewall.

Sample 5 - Mg-Ca- HCO_3

The water sample was collected from the steel pipe which was installed to drain water from the above excavations. The sampling point is at 102 m below ground surface and the mining area is currently mining a UG2 reef band. Upon collection, the water had no smell or odour and its flow rate was very high with an average of 125 ml/s. The water type for this sample is magnesium-calcium-bicarbonate. Bicarbonate is the most dominant anion at 500 mg/l whilst magnesium is the most dominant cation at 129 mg/l. Like most of the groundwater samples in the area, this sample plots in the same position as the groundwater samples on the piper plots (Refer to figure 5.15, main and insert). The pH is 7 with an EC value of 111 mS/m and the recorded TDS is 878.27mg/l.

This sample has a similar chemical signature like the most groundwater samples around the RBplat area (Figure 5.15). The excavation is also amongst the closest to the aquifer as it is 50 m below the aquifer. Based on the strong similarities between the hydrochemistry of this sample and the groundwater as well as the close distance to the aquifer, it is assumed that the source is meteoric groundwater which has interacted with ferromagnesium rocks that

contributed magnesium and calcium ions. The assumption is proved by the Gibbs plot where the sample plots on the water-rock interaction field.

Sample 6 - Na-Cl-HCO_3

The water sample was collected from underground tap water which is used for drinking. The tap is made from a water pipe with a rusted metalhead. The tap filled a 250 mm bottle in 2 seconds. The water was clear in appearance with no smell. The water sample was collected to be used as a standard reference to investigate if other water intersections are due to a leak.

From all the 6 samples collected from underground, the tap water has the lowest pH value of 6.52 and the lowest EC value of 1. 82 mS/m. The TDS content of this water was recorded at 585.85 mg/l which is also the lowest of the six samples and suggests that the water is fresh. All the major ions and tested metals indicate that the water is fresh and excellent for drinking. The sample had a second-highest concentration of 21 µg/l following sample 1.

The Gibbs plot on figure 5.16 indicates water-rock interaction as a dominant process that influenced the water chemistry of samples 1, 2 and 5 while sample 5 indicates evaporation as a process that influenced the water chemistry.

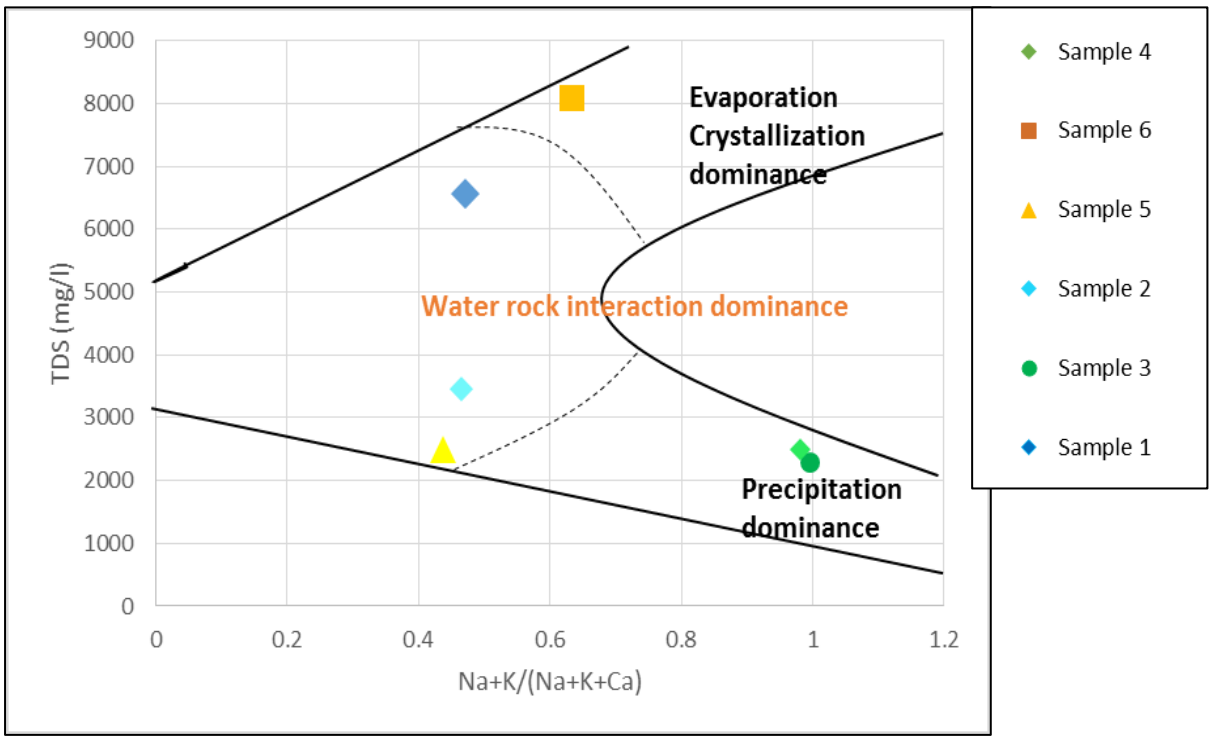

Figure 5.16: Gibbs plot of 6 water samples collected from the underground north shaft.

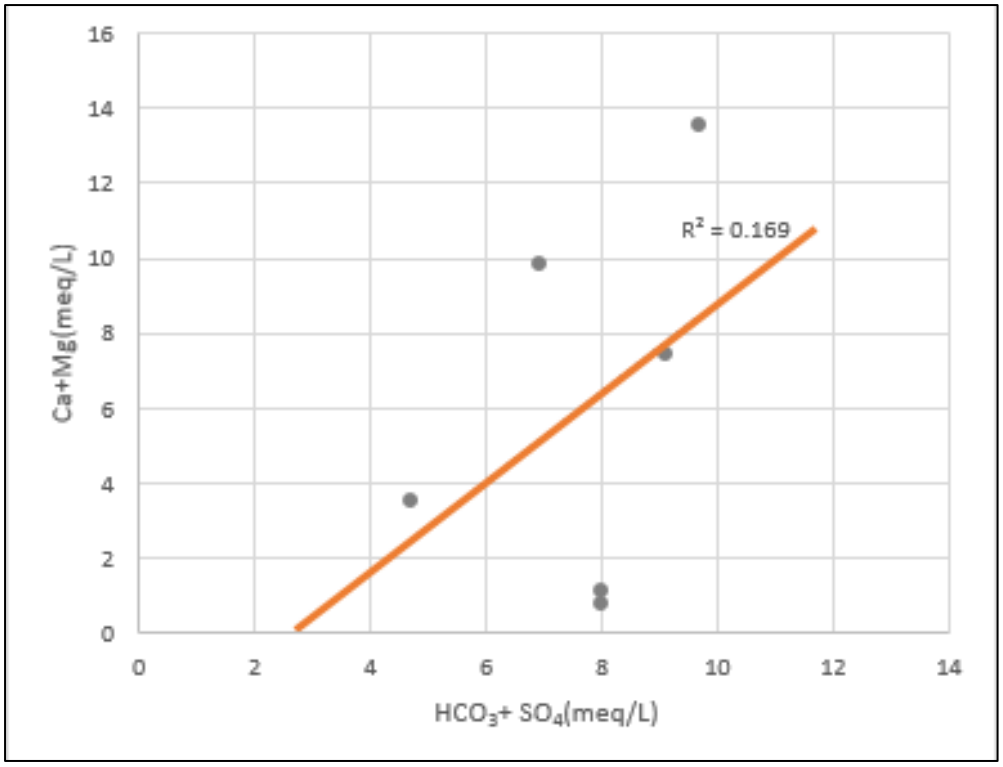

Figure 5.17: Ca+Mg vs HCO_4 +SO_4 plot for the 6 samples collected from underground North shaft.

5.4.2 Environmental Isotopes

Stable Isotopes (δ^2H and $\delta^{18}O$) were used to determine the source of water that ingresses into the underground working places. Six samples, which were collected from the north shaft underground were tested for deuterium and oxygen 18 isotopic compositions. Table 5.7 shows the isotopic composition, standard deviation, and the d-excess of the 6 samples. The d-excess is an indicator of how far the moist air mass has travelled from the source of vapour, therefore, the further it is from the source, the lower the d-excess. Groundwater whose source of moisture is from regional circulation tends to have low d excess (Geyh, 2000; Fitts, 2002; Zhu and Anderson, 2002). A general observation is that all the samples are depleted in both oxygen-18 and deuterium. From the six samples, samples 2 and 6 have a similar isotopic signature. They have the lowest d-excess and the same results for δ^2H and $\delta^{18}O$.

Table 5.7: Stable isotopic results of samples collected at the North Shaft. The results are of deuterium and oxygen 18 together with their standard deviations and d-excess.

Sample ID	$\delta^{2}H$ (‰)	± ^{2}H StDev (‰)	$\delta^{18}O$ (‰)	± ^{18}O StDev (‰)	d-excess
Sample 4	-30.1	0.2	-5.26	0.0	12.0
Sample 6	-9.8	0.3	-1.62	0.1	3.2
Sample 5	-26.5	1.3	-5.09	0.2	14.3
Sample 2	-9.8	1.6	-1.60	0.1	3.0
Sample 3	-30.5	0.4	-5.19	0.1	11.0
Sample 1	-27.6	0.2	-5.20	0.1	14.0

Based on the d excess results in Table 5.7, samples 6 and 2 are from a source whose moisture is from regional circulation. Samples 1, 3, 4 and 5 are from a source whose moisture is from local circulation. The vast variation between the d-excess of samples 2 and 6 relative to Samples 1, 3, 4 and 5 is a further indication of different moisture sources between the two groups.

The d-excess of samples 2 and 6 are 3‰ while the d-excess of samples 1, 3, 4 and 5 range between 11‰ and 14.3‰. These values give a further indication that the original moisture source of samples 2 and 6 formed in high temperature and low humidity environment. The further migration of samples 2 and 6 from the local meteoric water line as well as their low d-excess and isotopic enrichment are all linked to a moisture source, which formed during summer.

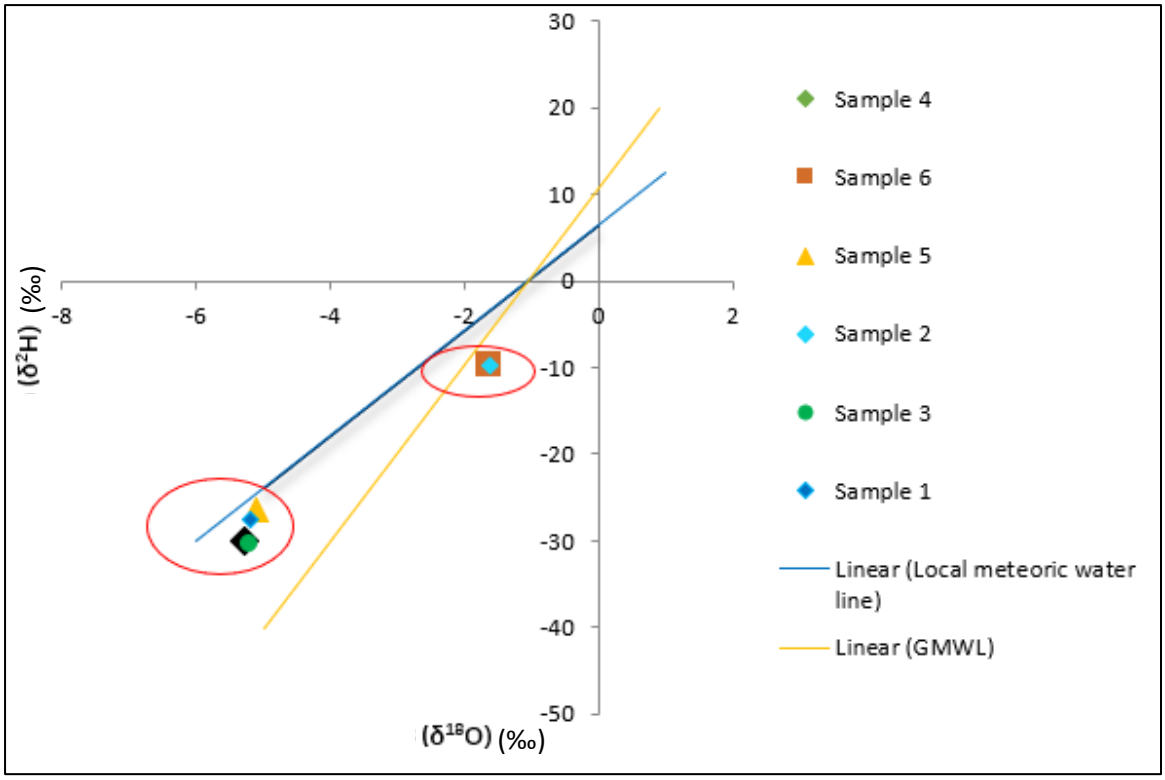

Figure 5.18: Correlation plot of oxygen-18 and deuterium in relation to the PMWL and GMWL.

The isotopic composition results in Table 5.7 are presented in Figure 5.18 and they are plotted against the Pretoria Meteoric Water line (PMWL) and the Global Meteoric water line (GMWL). The regression line of the GMWL is $\delta D = 8\ \delta^{18}O + 10$ ‰ (Craig, 1961) and the regression line for PMWL is $\delta D = 7.6\delta^{18}O + 7.2$ ‰ (Abiye et al., 2015). Relative to the PMWL, all samples plot below the line in 2 clusters. One cluster, which is less depleted plots below and far from the line, while the second cluster plots very close to the PMWL.

The isotopic composition of water is guaranteed to remain the same unless the water has undergone significant mixing or evaporation (Clark and Fritz, 1997). Sample 2 and 6 that represents cluster 2 exhibits a deviation from the local meteoric water line. The two samples plot below the PMWL and this indicates an effect of significant evaporation and mixing. These two samples contain more evaporated water than others, their recharge could have taken place in warmer seasons as compared to others. The samples plot far from the PMWL because they do not exhibit the same characteristics as the local precipitation. Samples 1, 3, 4, and 5 display a different signature from samples 2 and 6. The four samples are clustered very close to the PMWL, and this indicates a direct influence of local rainfall. The different isotopic signatures of the two identified clusters suggest that the samples have undergone different hydrogeological processes.

The minimal impact of evaporation on the samples 1, 3, 4 and 5 plotting along the PMWL can be attributed to the presence of multiple fractures that allow faster percolation of rainwater before immense evaporation can take place (Chirenje et al., 2014). Sample 2 and 6 have undergone multiple purification processes during which there is fractionation and the original isotopic signature could be altered.

Samples 2 and 6 exhibit different isotopic compositions from the four samples collected from underground workings and these samples present a similar isotopic composition to the local precipitation. This confirms that the municipal supply underground had no leaks and the four samples are from local precipitation.

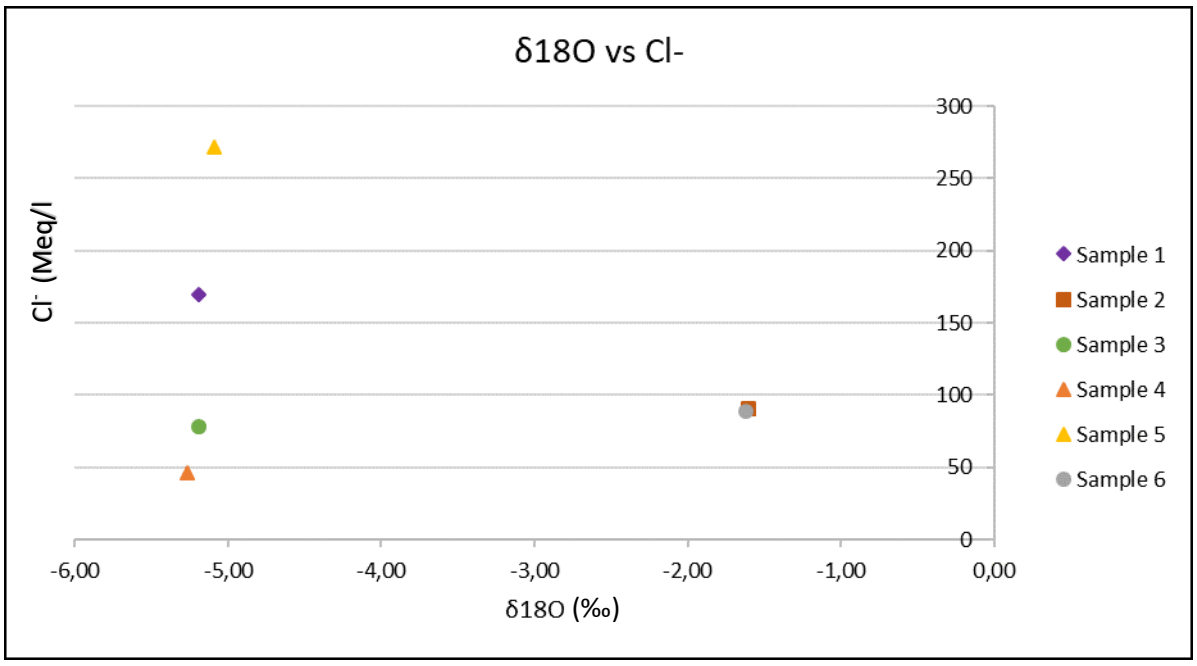

Figure 5.19: δ ^{18}O versus Chlorine ions for the 6 samples

Figure 5.19 shows the relationship between oxygen 18 and chloride ions. The chloride content has an increasing trend, while ^{18}O is the same for samples 1, 3, 4 and 5. The ^{18}O of the four samples suggest the water is from a similar moisture source while chloride could be contributed from the host rocks. The samples collected at high elevations have high chlorine while the samples collected at lower elevations have low chloride ions. Sample 2 and 6: similar cl source due to evaporation.

CHAPTER 6
CONCLUSION AND RECOMMENDATIONS

6.1 Conclusion

This research revealed Mg-HCO_3 to be the most dominant water type with over 50% of the tested water samples having the same water type. Mg-SO_4 is the second most dominant water type and it was noted in the water samples, which were collected near tailing facilities around the mine. The magnesium ions were the most dominant cations, and this was attributed to the interaction between water and the host rocks. The dominant anion in the water was bicarbonate. Since this environment is not calciferous, the source of bicarbonate was deduced to be the dissolution of carbon dioxide in water that produces carbonic acid that further dissociates to form it. The high levels of sulphate around tailings are linked to leachate migration from the surface to the aquifer. A few samples came out to be mixed, and the mixing was between fresh meteoric source and recent recharge water affected by evaporation. A different mixing process was also between fresh meteoric groundwater and sulphide bearing leachate.

Bivariate plots and molar ratios revealed the presence of silicate weathering to be one of the prime processes contributing to major ions to the groundwater. Even though molar ratio calculations and bivariate plot analysis indicated that feldspar weathering played a major role in the chemical composition of the groundwater, this could not be proved with saturation index calculations because SiO_2 was not analysed.

Due to the area being semi-arid and having high temperatures, evaporation was found to be among the processes that influenced the ion chemistry in the water around the mine. The saturation index results revealed calcite precipitation to be taking place in the groundwater and it is observed in the fractures around the mine.

A conclusion drawn from the North shaft underground investigation was that samples 2 and 6 are not isotopically related to samples 1, 3, 4 and 5. Therefore, this confirms that there is no leak from the municipal pipes underground. Samples 1, 3, 4 and 5 which were collected from underground intersections are of meteoric origin from the local rainfall. The samples also have an isotopic composition which plot very close to the PMWL. The water ingress into the mine is therefore originally local precipitation which makes its way to the mining areas through geological fractures and opening.

6.2 Recommendations

- A further hydrogeological study must be conducted around the tailing facilities to see the extent and depth at which the groundwater is affected by the material stored at the tailings.

- For the groundwater monitoring data retrieved from the mine database, the reliability test of most of the samples was unreliable. The sampling and analysis procedures currently used should be monitored and audited to improve the reliability of the data. SiO_2 to be analysed for in the next project.

- In future, to have more reliable findings, sampling for bacteria as well as isotopic tests should be incorporated in the study.

REFERENCES

Ahmed, S. and Saxena, V. (2001): Dissolution of fluoride in groundwater: A water rock interaction study. *Environmental Geology*, **40**(9):1084–1087. DOI 10.1007/s00254-002-0672-2

Atangana, A., Ahokpossi, P. and Vermeulen D. (2017): Hydrogeochemical characterizations of a platinum group element groundwater system in Africa. *Journal of African Earth Sciences,* **138**:348-366. https://doi.org/10.1016/j.jafrearsci.2017.11.032

Appelo, C. and Postma, D. (2005): Geochemistry, groundwater and pollution. (2nd edition). Rotterdam: Balkema.

Appelo, C. and Parkhurst, D. (2016): Description of input andexamples for PHREEQC Version 3-A computer program for speciation, batch-reaction, one-dimensional transport, and inverse geochemical calculations. Department of the Interior, U.S.

Brown, C. (2012): Applied multivariate statistics in geohydrology and related sciences. Springer Science & Business Media.

Brusseau, M., Carroll, K., Carreon-Diazconti, C., Johnson, B. and Miao, Z. (2011): Sulfate reduction in groundwater: Characterization and applications for remediation. *Environmental Geochemistry and Health*, **34**(4):539-550. DOI: 10.1007/s10653-011-9423-1

Cawthorn, G. (2010):The platinum group element deposits of the Bushveld Complex in South Africa. Platinum Metals Rev., 2010, **54**(4):205–215. DOI:10.1595/147106710x520222

Cawthorn, G. (2006): Origin of the Pegmatoidpyroxenite in the Merensky Unit, Bushveld Complex, South Africa.

Cherry, A. and Freeze, A. (1979): Groundwater. Prentice Hall.

Chilton, P. and Foster, S. (1995): Hydrogeological characterisation and water-supply potential of basement aquifers in tropical Africa. *HYJO* **3**:36–49. https://doi.org/10.1007/s100400050061

Chenini, I., Farhat B. and Mammou, A. (2014): Identification of major sources controlling groundwater chemistry from a multi-layered aquifer system. Vol.26 N0.4.

Clark, I. and Fritz, P. (1997): Environmental Isotopes in Hydrogeology. Lewis Publishers, New York, 1 – 352 pp

Clark, I. (2015): Groundwater geochemistry and isotopes. Boca Raton, FL: CRC Press.

Crawford, J. (1999): Geochemical modelling: A review of current capabilities and future directions. Royal Institute of Technology.

Das, P. and Karmakar, H. (2012): Impact of mining on ground and surface water. *International Mine Water Association*,Orrisa, India.

Davis, F., Kresse, M., Kim, B., Steele, K. and Fazio, J. (2008): Inverse geochemical modelling of groundwater evolution with emphasis on arsenic in the Mississippi River Valley alluvial aquifer, Arkansas (USA), Environmental Dynamics Program and Department of Geosciences, University of Arkansas, Fayetteville, AR 72701, USA.

Delport, R. (2012): Hydrogeological investigation for the proposed expansion to tailing dam No. 6 at Western Platinum Mines Limited.

DWAF, (1996b): South African Water Quality Guidelines. Volume 4: Agricultural Use: Irrigation 2nd Edition. Holmes, H (Eds), Department of Water Affairs and Forestry.

Elgano, L. Kannan, R. (2007): Rock-water interaction and its control on chemical composition of groundwater. In: Sarkar, D., Datta, R., and Hannigan, R. (eds.), Developments in Environmental Science. Elsevier, Chapter 11, p. 229–243.

Fitts, C. (2002). Groundwater Science. Academic Press Publishers, Amsterdam, 1 – 449 pp.

Fitts, C. (2013): Groundwater Science 2nd edition, Academic Press, University of Southern Maine, Gorham, USA.

Geyh, M. (2000). Environmental isotopes in the hydrological cycle: Principles and applications. International Atomic Energy Agency and United Nations Educational, Scientific and Cultural Organization, **vol. 4**, 311 – 424 pp.

Goncharov, P. Lapin, Y. Shneerson, M. Sokolskaya, I. Tatarnikov, V. (2004): Treatment of Platinum Flotation Products. Platinum Metals Rev., 2004, 48, (3)

Gupta, P. and Singhal, B. (2010): Applied hydrogeology of fractured rocks 2nd edition, Department of Earth Sciences, Indian Institute of Technology, Roorke, India.

Hiscock, K. (2005): Hydrogeology: Principles and practice, Cowly Road, Oxford, United Kingdom: Blackwell Publishing.

Hounslow, A. (1995). Water quality data: Analysis and interpretation. New York: Lewis Publishers, 1 – 416 pp.

Hounslow, A. (2018): Water quality data: Analysis and interpretation. CRC Press, Technology & Engineering, London, New York.

Hollard, M. and Rossouw, T. (2016): BCR minerals – Groundwater impact assessment, Delta H, Delh.2015.045-1.

Imrie, S. Mabenge, B., Nyembe, M. and Skinner, S. (2014): Styldrift L shape tailings disposal site: Hydrogeological Specialist study. SRK Consulting.

Jalali, M. (2007): Assessment of the chemical components of Famenin groundwater, Western Iran. Environmental Geochemistry and Health, **29 (5)**, 357 – 374 pp.

Jalali, M. (2009): Geochemistry characterization of groundwater in an agricultural area of Razan, Hamadan, Iran. Environmental Geology, 56(7):1479-1488. DOI: 10.1007/s00254- 008-1245-9

Kura, N. Ramli, M. Sulaiman, W. Ibrahim, S., Aris, Z. and Mustapha, A. (2013): Evaluation of factors influencing the groundwater chemistry in a small tropical island of Malaysia. International Journal of Environmental Research and Public Health, **10 (5)**, 1861 – 1881 pp.

Kinnaird, J, White, J. and Schurmann, L. (2005): Multiphase emplacement of the Platreef, northern Bushveld, South Africa. Abstract. 10th Platinum Symposium, Oulu, Finland, 7-9 August 2005

Kinnaird, J. (2016): The Bushveld large province. School of Geosciences, University of the Witwatersrand.

Lenkoe-Magagula, K. (2013): Groundwater impact assesment-18 Shaft, SLR- Global Environmental Solutions.

Ligavha-Mbelengwa, L. (2017): Investigation of the groundwater hydrogeochemistrycharacteristics in Beaufort West, South Africa. MSc dissertation, University of the Free State, South Africa.

Masindi, K. and Abiye, T. (2018): Assessment of natural and anthropogenic influences on regional groundwater chemistry in a highly industrialized and urbanized region: Acase study of the Vaal River Basin, South Africa, School of Geosciences, University of the Witwatersrand.

MacCaffrey, L. (1998): Distribution and causes of high fluoride in the Western Bushveld area, South Africa. University of Cape Town.

Nazzal, Y., Ahmed, Al-Arifi, N, Ghrefat, H., Zaidi, F, El-Waheidi, M, Batayneh, A. and Zumlot, T. (2014): A pragmatic approach to study the groundwater quality suitability for domestic and agricultural usage, Saq aquifer, Northwest of Saudi Arabia. Environmental Monitoring and Assessment, 186:8:4655-4667. DOI: 10.1007/s10661-014-3728-3

Padiachy, P. (2015): RBplat Annual MR Model Report. Unpublished Internal Report.

Schouwstra, R.P., Kinloch, E.D. and Lee, C.A. (2000): A short geological review of the Bushveld Complex.Platinum Metals Review, **44**(1):33-39.

Schuster, P.F. (2013): Quality assurance. Water chemistry. USGS.

Swaminathan, G. and Venkatesan, G. (2009): Review of chloride and sulphate attenuation in groundwater nearby solid-waste landfill sites. *Journal of Environmental Engineering and Landscape Management*.17:1, 1-7, DOI: 10.3846/1648-6897.2009.17.Ia-Ig

Titus, R., Walters, B., and Witthuser, K. (2009): Groundwater and Mining In The Bsuveld Complex, South Africa.

Van Der Merwe, T. (2015): Integrated Environmental Authorization process for the proposed extension of the existing BafokengRasimone Platinum Mine, tailings storage facility and associated infrastructure, North West Province. SRK Consulting, Pretoria South Africa.

Van Coller, A. (2013): Open pit flooding as a post closure option: A geochemical approach. University of the Free State.

Villers du Preez, L. (2018): Investigating the different support methods for various geological structures encountered in hard rock mining within the Eastern Limb of the Bushveld Igneous Complex, South Africa

WHO (World Health Organisation) (2011): Guidelines for drinking-water quality. (4th edition). (NLM classification: WA 675). Geneva, Switzerland.

Zaidi, F., Nazzal, Y., Jafri, M. K., Naeem, M. and Ahmed, I.(2015): Reverse ion exchange as a major process controlling the groundwater chemistry in an arid environment: A case study from Northwestern Saudi Arabia. Environmental Monitoring and Assessment, 187(607):1-18. DOI: 10.1007/s10661-015-4828-

Zhu, C. and Anderson, G. (2002). Environmental Applications of Geochemical Modelling. Cambridge University Press, New York, USA, 1 – 300 pp.